Signal Optimised Wavelet Transforms for Signal Compression

A Project Report
Submitted in partial fulfilment of the
requirements for the Degree of
Master of Engineering
in
SIGNAL PROCESSING

by

Mathews Jacob

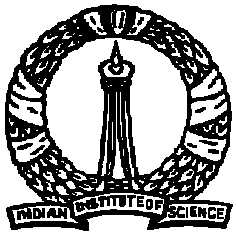

Department of Electrical Engineering and Department of Electrical Communication Engineering
Indian Institute of Science
BANGALORE – 560 012

APRIL 1999

Contents

List of Figures

Acknowledgements

I would like to thank my project guide, Dr.G.V. Anand, Professor in ECE (Electrical Communication Engineering) for his invaluable guidance throughout the course of the project. He always found time to discuss the technical matter and provide the necessary suggestions and encouragement. I would also like to thank Prof. A.Makur and Prof. K.Rajgopal for their valuable comments.

I would also like to thank the members of the Acoustics Lab (Abhilash.G, Lakhsmipathi, Rakesh Prasad and Arunachalam) for their help and support.

I would particularly thank Krishnagiri.V for all the help he has offered towards the completion of my thesis.

Abstract

Transform coding is a popular technique adopted for lossy signal compression, which makes use of the energy compaction in the transform domain. The energy compaction is dependent on the optimality of the transform to the given signal. Wavelet transform is ideally suited for adaptive transform coding as the basis vectors are related to each other and the representation of the basis vectors itself becomes simple unlike other transforms.

As the coding gain is proportional to the energy compaction, a wavelet is termed to be optimum to a signal if it can approximate the signal better at a coarser scale, as compared to other wavelet transforms. We introduce a scheme which derives a multi-scaling function adapted to a given signal. The so derived multi-wavelet basis, will approximate the given signal better at a coarser scale, as compared to other bases in the particular class of wavelets considered.

We introduce a multi-wavelet, that is better as compared to conventional wavelet basis in the representation of collage error in Fractal Image coding scheme. This basis, will restrict the block edge details of the collage error, to a coarser scale, which a conventional wavelet basis would spread to all scales. Hence the truncation of the coefficients at finer scales for coding gain, will not cause the block edge details to be lost which would cause blockiness in the reconstructed image, which is very disturbing. This scheme also permits us to provide lesser bits at block edges where the discontinuity is less, and provide those bits for the representation of natural edges of the image. As this new transform separates the details having different perceptual implications to different bands, images can be reconstructed at a better perceptual quality.

We also consider a generalisation of the conventional Multi-Resolution Axioms. A filter bank structure for the decomposition of signals in this basis was also derived. However, this generalisation was later found to be a special case of a more general multi-wavelet basis. This scheme with orthogonality constraint yields wavelets with very low approximation order, and high fractal characteristics.

Chapter 1

Introduction

The approximation of a signal using minimal number of parameters is an important problem in many engineering applications like Signal compression, Matched filtering etc. One popular approach to solve this problem is the linear transformation with zonal sampling, where signal is approximated by the projection onto a finite dimensional subspace of the signal space, where the most of the desired information of the signal is concentrated. The desired information can be quantified by the energy of the signal, or by some perceptual measure. The popularity of this technique is mainly due to the mathematical tractability and the ease of introducing perceptual measures in the approximation of signals like audio, images etc.

The choice of the optimal subspace to which the signal is projected, so that the approximation results in minimal loss of useful information, is highly dependent on the characteristics of the signal considered and the norm of the error to be minimised (which is dependent on the perceptual measure considered). The choice of the subspace, which in-turn is determined by the choice of the transform, can be posed as a mathematical problem and is solved in the case of Random Stationary signals . The solution with the energy of the error in approximation as the performance measure, is the Karhunen Loeve Transform(KLT), where the basis vectors of the transform are the eigen vectors of the Auto-correlation matrix. In zonal sampling, the eigen vectors with maximum eigen value are chosen, and hence the subspace turns out to be the space where maximum energy of the signal is concentrated. The above solution is based on the assumption that the signal considered is stationary, which is not true with most of the practical signals. This calls for the adaptation of the transform to the local statistics of the signals.

In signal compression applications, such a scheme where the transform is adapted to the local statistics of signals, is not profitable due to the large overhead in the transmission of the basis vectors. However if the transform basis vectors are constrained to be related to each other, as in the case of the Wavelet Transform, the overhead is not large as above. In the wavelet transform the basis vectors are the dilates of each other and hence, from one basis vector all the basis vectors can be generated. So such a transform is ideally suited for a signal adapted transform for signal compression applications.

Wavelet transform has attracted the attention of many researchers both in theoretical and applied areas in the recent past. As compared to other transformations, the basis vectors of the wavelet transformation, are localised in time and frequency, while most of the other transformations are not localised in time. One of the reasons for its success could be the constant "Q" nature of the basis vectors, being similar to our perceptual mechanisms. Wavelet theory, witnessed a brisk activity in signal processing since the work of Mallat[17] in 1989, where he introduced the relation between Multi-Resolution Analysis(MRA) and wavelet analysis.

A relation between fractals and Multi-resolution analysis can easily be seen. While MRA generates signals of coarser resolutions from signals of higher resolutions, a fractal generator (eg. Fractal interpolator) generates signals at finer resolutions from that of coarser resolutions. Hence the fundamental operator of an MRA can be seen as an inverse operator of the fundamental operator of a fractal generator, at-least for some simple operators of this class.

The wavelet spaces that satisfy the Multi-resolution axioms, have a scaling function that is obtained by the iteration of the two-scale relationship. The two-scale relationship is nothing but the Iterated Function System(IFS) which was suggested by Barnsley[16] in 1985, for the generation of fractal objects.

The rest of the thesis is be organised as mentioned below.The Chapter 2 gives a review of wavelet theory with the main focus being on its applications to signal approximation and compression. In the third chapter an extension of the conventional multi-resolution analysis is discussed and a filter bank implementation of the above analysis is presented. The approximation properties of the above analysis is also discussed in the above chapter. The fourth chapter introduces a new multi-wavelet which localises the details corresponding to the block edges in the collage error in a Fractal Image compression scheme to the lower resolution spaces. The implementation details of a scalable fractal image coder based on the above multi-wavelet are also given in this

chapter. In Chapter 5, the optimisation of a multi-wavelet to a given signal, assuming it to be generated by a fractal generator, is discussed. Conclusions and suggestions for further work is presented in Chapter 6.

Chapter 2

Signal Compression Using Wavelets

2.1 Introduction

For a long time Fourier analysis was a very useful technique for the analysis of a signal. But this technique has certain disadvantages as well. The basis functions (complex exponentials) have an infinite support, and hence when we deal with quasistationary signals like speech where the frequency content of the signal varies with time, the temporal information in the signal is lost. Wavelet transform, which has basis functions localised in time, retains this temporal information. Hence for dealing with nonstationary signals like speech, wavelet transform has certain advantages over the conventional transforms.

In this chapter a brief review of wavelet theory with focus on its application to approximation of functions is presented.

2.2 The Discrete Wavelet Transform

The discrete wavelet transform of a signal is defined as the the mapping $T : L^2(\Re) \rightarrow L^2(\Re)$ of the form

$$(Tf)_{n,k} =< f, \psi_{n,k} >= \int_{\Re} f(x)\psi_{n,k}(x)dx, \tag{2.1}$$

where $\psi_{n,k}$ is

$$\psi_{n,k}(x) = a^{\frac{n}{2}}\psi(a^{-n}x - kb) \tag{2.2}$$

Here the function ψ is called as the mother wavelet and satisfies the admissibility condition given by,

$$0 \ < \ \int_{-\infty}^{\infty} \frac{|\hat{\psi}(\omega)|^2}{\omega} d\omega \ < \ \infty, \quad \text{where} \tag{2.3}$$

$\hat{\psi}(\omega)$ is the fourier transform of the function $\psi(x)$. This condition implies that

$$\int_{-\infty}^{\infty} \hat{\psi}(\omega) d\omega = 0 \tag{2.4}$$

It also imposes an upper bound on the asymptotic decay of the Fourier transform of the wavelet as the frequency $\omega \to \infty$.

Wavelet theory became popular in signal processing, after the work of Mallat[17] where he introduced the relationship between wavelet analysis and Multi-resolution analysis. This scheme gives a systematic approach for the understanding of wavelet theory and the construction of wavelets for practical applications.

2.3 Multi-resolution Analysis

Definition 2.3.1 *A multi-resolution analysis of $L^2(\Re)$ is a sequence of closed subspaces $\ldots, V_{-1}, V_0, V_1, V_2, \ldots$ such that*

(M1) $V_n \subset V_{n-1}$
(M2) $\bigcup_{n=-\infty}^{\infty} V_n$ *is dense in* $L^2(\Re)$ *and* $\bigcap_{n=-\infty}^{\infty} V_n = 0$
(M3) $f(x) \in V_n \iff f(2x) \in V_{n-1}$
(M4) $f(x) \in V_0 \iff f(x-k) \in V_0, \quad \forall k \in Z$
(M5) There exists an isomorphism $\mathbf{I}$ *from* V_0 *onto* $\ell^2(Z)$ *which commutes with the action of* Z

In (M5), the action of Z over V_0 is the translation of functions by integers whereas the action of Z over $\ell^2(Z)$ is the usual translation. The approximation of a function $f(x)$ at resolution j is the orthogonal projection of $f(x)$ on V_j .

The operator $\mathbf{I}$ is an isomorphism from V_0 to $\ell^2(Z)$. Hence there exists a function $g(x)$ which satisfies

$g(x) \in V_0$ and $\mathbf{I}(g(x)) = e(n)$, where

$$\begin{aligned} e(n) &= 1 \quad if \quad n = 0 \quad and \\ &= 0 \quad if \quad n \neq 0. \end{aligned}$$

Since $\mathbf{I}$ commutes with translation of integers,

$$\mathbf{I}(g(x-k)) = e(n-k)$$

The sequence $e(n-k)_{k \in Z}$ is a basis of $\ell^2(Z)$, and hence $(g(x-k))_{k \in Z}$ is a basis of V_0. An arbitrary function $f(x) \in V_0$ can be expressed in terms of these basis functions as

$$f(x) = \sum_{k=-\infty}^{\infty} a_k . g(x-k) \tag{2.5}$$

where $(a_k) \in \ell^2(Z)$. Taking the Fourier transform on both the sides, interchanging the summation and integration(which is permitted as Fourier transform is a continuous operator) and by Lemma 3.1 of [9] we get

$$\hat{f}(\epsilon) = A_f(\epsilon) . \hat{g}(\epsilon) \tag{2.6}$$

where $A_f \in L^2_{(0,2\pi)}$ and is given by $A_f(\epsilon) = \sum_{k=-\infty}^{\infty} a_k . \exp(ik\epsilon)$. We can also say that $f \in V_0$ only if (2.6) holds for some $A_f \in L^2_{(0,2\pi)}$.

The above mentioned basis functions form a Reisz basis for the above spaces, but they need not be orthogonal. Orthogonality of the basis functions is certainly a desirable feature. The paper by Heijmans[9] is a consolidated work on this topic.

2.4 Approximation Properties of the Wavelet Transform

Assume that the orthogonal scaling functions are given by $\phi(x)$. In this case, an arbitrary function $f(x) \in L^2(\Re)$ may be approximated by its projection onto the space V_j, given by $\sum_k b_k \phi(2^j x - k)$. The accuracy of this approximation increases as the value of "j" increases. The asymptotic accuracy of the representation for any signal, that is

differentiable more than p times, is decided by the number of polynomials $1, x, \ldots, x^{p-1}$, that can be exactly represented by a combination of the translates of $\phi(x-k)$. The approximation error will decrease as h^p as $h \to 0$, where $h = 2^{-j}$. This is proved as follows . Any p times differentiable function $f(x)$ can be written as

$$f(x) = f(x^*) + f^{'}(x^*)(x-x^*) + \frac{f^{''}(x^*)(x-x^*)^2}{2} + \ldots + O(||x-x^*||^p) \tag{2.7}$$

In the above equation, $f(x^*)$ corresponds to the value of the function at the grid points $(2^{-j}k), k \in Z$ and x is an a intermediate point. At a particular resolution, the error in the approximation is proportional to $O(||x-x^*||^p)$, where the term $(x-x^*)$ is proportional to the distance between the grid points which at a resolution "j" is given by 2^{-j}. Hence the above result. This result gives the asymptotic decay of the upper bound of the error due the truncation of the wavelet fine scale coefficients. It is to be noted that this is valid only for smooth functions which are p times continuously differentiable. For a more rigorous proof refer to [3]

If a wavelet decomposition has an approximation order of p, the polynomials $1, x, \ldots, x^p$ can be represented exactly by the translates of the scaling function. This in-turn implies that the the moments of the wavelet and scaling functions are as follows.

$$M_p = \int_{-\infty}^{\infty} x^p.\phi(x) \neq 0 \tag{2.8}$$

$$N_p = \int_{-\infty}^{\infty} x^p.\psi(x) = 0 \tag{2.9}$$

Here $\psi(x)$ is the mother wavelet.

As the scaling function is the basis of the MR space, it satisfies the twos scale relation

$$\phi(x) = \sum_k c_k.\phi(2x-k) \tag{2.10}$$

The wavelet function satisfies the equation

$$\psi(x) = \sum_k d_k.\phi(2x-k) \tag{2.11}$$

The coefficients c_k are called as the mask of the scaling function. In the orthogonal

case, the coefficients d_k are given by

$$d_k = (-1)^k . c_{-k+1} \tag{2.12}$$

The condition (2.9) implies that the Fourier Transform of the wavelet $\hat{\psi}(\omega)$ has a root of multiplicity N at $\omega = 0$. As $\hat{\phi}(0) \neq 0$, the above condition implies that $D(\omega)$, which is the Fourier transform of the sequence d_k, has a root of multiplicity N at $\omega = 0$. The condition $\hat{\phi}(0) \neq 0$, is implied by the "partition of unity" condition which has to be satisfied for the MR spaces defined by the scaling function, to satisfy (M2). This condition along with equation(2.12) implies that the filter transfer function $C(\omega)$ (Fourier Transform of the sequence c_k), has N roots at π. The above conditions imply that the filter $C(\omega)$ can be factorised as

$$C(\omega) = \left(\frac{1 + e^{-i\omega}}{2}\right)^N K(\omega), \quad \text{with } K(0) = 0 \text{ and } K(\pi) \neq 0. \tag{2.13}$$

The above factorisation was the starting point of the construction of compactly supported wavelets[11]. Daubechies has shown in [10] that the above factorisation leads to an upper bound on the asymptotic decay of $\hat{\phi}(\omega)$ as $\omega \to \infty$, subject to some constraints on the function $K(\omega)$. This implies an upper bound on the asymptotic decay of the function $\hat{\psi}(\omega)$. The condition(2.9) indicates the decay of the function $\hat{\psi}(\omega)$ as $\omega \to 0$. These properties together imply that the wavelet becomes more band-limited as the order of approximation increases. The increase in the order of approximation is not without any price to pay. As the order of approximation increases, the support of the function in the time domain increases.

Daubechies have shown in [12] that a function cannot simultaneously satisfy all the desirable conditions for signal representation as,

- Orthogonality.
- Symmetry/Linear phase analysis filters.
- Short support.
- High approximation order.

The Daubechies wavelets, which are orthogonal wavelets with the shortest possible support with a particular approximation order, are orthogonal but not symmetric, and there exists a trade off between approximation order and support. This is the

motivation for the generalisation of the Multi-Resolution axioms to introduce multi-wavelets. It is seen that there exist multi-wavelets that satisfy all the above desirable conditions. The next section briefly discusses the theory of multi-wavelets.

2.5 Multi-wavelet Analysis of $L^2(\Re)$

Multi-wavelets are obtained by the generalisation of the conventional Multi-resolution axioms as below

Definition 2.5.1 *A multi-resolution analysis of $L^2(\Re)$ is a sequence of closed subspaces $\ldots, V_{-1}, V_0, V_1, V_2, \ldots$ such that*

(M1) $V_n \subset V_{n-1}$
(M2) $\bigcup_{n=-\infty}^{\infty} V_n$ *is dense in* $L^2(\Re)$ *and* $\bigcap_{n=-\infty}^{\infty} V_n = 0$
(M3) $f(x) \in V_n \iff f(2x) \in V_{n-1}$
(M4) $f(x) \in V_0 \iff f(x-k) \in V_0$ *for all* $k \in Z$
(M5) There exists an isomorphism $\mathbf{I}$ *from* V_0 *onto* $\ell^2(Z^N)$ *which commutes with the action of* Z

It is to be noted that only the axiom (M5) is changed, while the others remain the same. The new set of axioms imply that there exist scaling functions $\phi_1, \phi_2, \ldots, \phi_N$ such that the translates of these functions will span the multi-resolution spaces. Now the new two-scale relationship will be as under.

$$\phi_i(x) = \sum_j \sum_k c_{i,j}(k)\phi_j(2x-k) \tag{2.14}$$

Correspondingly, the wavelet space will be spanned by the translates of N functions which are obtained as

$$\psi_i(x) = \sum_j \sum_k d_{i,j}(k)\phi_j(2x-k) \tag{2.15}$$

The above equations can be written in the matrix form as

$$\phi(x) = \sum_k C_k.\phi(2x-k) \tag{2.16}$$

$$\psi(x) = \sum_k D_k.\phi(2x-k) \tag{2.17}$$

In the above equations, C_k and D_k are matrices which are given as $[C_k]_{i,j} = c_{i,j}(k)$ and $[D_k]_{i,j} = d_{i,j}(k)$ respectively. In the implementation of the above analysis, there will be multi-filters corresponding to scalar filters in conventional wavelet analysis. The multi-filters are N-input, N-output filters. In the conventional wavelet analysis of discrete signals(where we are provided with the samples of the actual signal), we assume the signal which we analyse to be a function, whose projection on the translates of the scaling function are the samples we have. However in multi-wavelet analysis, as a vector input is needed, we need to split the given signal onto different bands. This is done using a prefilter.

2.6 Approximation properties of Multi-wavelet Analysis

In multi-wavelet analysis also, as in the scalar wavelet case, we desire a good approximation order. This topic is discussed in depth in [2]. This section briefly discusses the results.

An approximation order of p implies that polynomials of order up to p can be represented in terms of the basis functions of the space V_0. Hence we can say that there exists row vectors $\overline{y}^j$ whose elements are y_k^j such that,

$$\sum_k y_k^j \phi(x+k) = x^j, \quad \text{for } j = 0, 1, 2, \ldots, p-1 \tag{2.18}$$

If we write $\overline{y}^j$ as $[\ldots, y_0^j, y_1^j, \ldots]$, then $y^j F(x) = x^j$., where

$$F(x) = [\ldots, \overline{\phi}(x-1), \overline{\phi}(x), \ldots]^T \quad \text{where} \tag{2.19}$$

$$\overline{\phi}(x) = [\phi_1(x), \phi_2(x), \ldots, \phi_N(x)] \tag{2.20}$$

Now it can be seen as,

$$y^j L F(x) = y^j F(\frac{x}{2}) = (\frac{x}{2})^j = 2^{-j} y^j F(x) \tag{2.21}$$

If the basis functions $\phi_i(x)$ are linearly independent, it can be seen that

$$y^j L = 2^{-j} y^j \tag{2.22}$$

The above equation implies that the vector y^j is the left eigen vector of the matrix L,

where $LF(2x) = F(x)$, and $L_{i,j} = c_{2i-j}$, with the eigen value 2^{-j}. The above mentioned analysis shows that an accuracy of p implies that the matrix L has p eigen values $1, \frac{1}{2}, \ldots, (\frac{1}{2})^{p-1}$. Moreover, the coefficients y_k^j being the projections of the function x^j on $\phi(x-k)$, there is a structure to these coefficients.

$$\begin{aligned} y^j F(x-l) &= (x-l)^j & (2.23) \\ &= \sum_{m=0}^{j} \binom{j}{m} (-l)^{j-m} y_0^m & (2.24) \end{aligned}$$

Hence

$$\begin{aligned} y^0 &= [\ldots, \ldots, u, u, u, \ldots, \ldots] \\ y^1 &= [\ldots, \ldots, v, v-u, v-2u, \ldots, \ldots] \\ y^2 &= [\ldots, \ldots, w, w-2v+u, \ldots, \ldots] \end{aligned}$$

The above eigen vectors along with p eigen values as mentioned above implies that the multi-wavelets have an approximation order of p. These conditions are modified to a compact form in [2] as,

Theorem 2.6.1 *Given the vectors $y_0^{(0)}, \ldots, y_0^{(p-1)}$, then $y^j L = 2^{-j} y^j$ iff the following two finite equations are satisfied for $j = 0, \ldots, p-1$.*

$$\begin{aligned} \sum_{m=0}^{j} \binom{j}{m} 2^m (-1)^{j-m} y_0^m A_{j-m} &= 0 & (2.25) \\ \sum_{m=0}^{j} \binom{j}{m} 2^m (-1)^{j-m} y_0^m S_{j-m} &= 2 y_0^j & (2.26) \end{aligned}$$

where

$$A_j = \sum_{k=0}^{N} (-1)^k k^j c_k \qquad \text{and} \qquad S_j = \sum_{k=0}^{N} k^j c_k \tag{2.27}$$

In terms of the symbol $M(\omega) = \frac{1}{2} \sum c_k e^{(-ik\omega)}$, the equations(2.27) are:

$$A_j = \frac{2}{(-i)^j} M^{(j)}(\pi) \qquad \text{and} \qquad S_j = \frac{2}{(-i)^j} M^{(j)}(0) \tag{2.28}$$

These conditions are applicable to scalar wavelets too in which the above conditions simplify to the condition of p zeros at π.

Chapter 3

Generalised Multi-resolution Analysis

3.1 Introduction

The relation between the conventional Multi-resolution Analysis(MRA) and the Wavelet Transforms was introduced by S.Mallat [17] in 1989. Since then, a large number of wavelet bases, which fall in this class were introduced. But certainly, the class of wavelet bases characterised by MRA is not complete (eg. Morlet wavelet cannot be characterised using MRA as it does-not have a scaling function). Conventional wavelets characterised using MRA have certain disadvantages as they cannot have a high approximation order, linear phase property, short support and orthogonality simeltaneously. If by extending the conventional Multi-resolution axioms, we can define a wider class of functions which have all the above mentioned properties simeltaneously it is very desirable.

In this chapter, we consider an extension of the conventional MR axioms to define a larger class of wavelets. The motivation is to generate more regular wavelets with a shorter support. The motivation for the scheme is explained below.

For a higher smoothness of the wavelet(and hence higher regularity), the decay of the scaling function in the Fourier domain has to be sufficiently high. As a scaling function is characterised by the two scale relationship (2.10), the asymptotic decay of the scaling function is decided by the decay of the filter transfer function $C(\omega)$. If we want to improve the decay of $C(\omega)$, it cannot be done without increasing the order of

the filter and hence the support of the scaling function. But if we have a multi-scale relationship as in equation(3.4), we can have a faster decay for the scaling function without the filters being constrained to have a fast decay by choosing $C(\omega)$ and $D(\omega)$ appropriately, as shown in figure(3.1). For this to happen the filters have to be low-pass and high pass respectively, so that the high-pass components of $C(\omega)\phi(\omega/2)$ will be cancelled by that of $D(\omega)\phi(\omega/4)$.

Hence, we can hope to have wavelets with a shorter support and a higher regularity, in this Generalised class of wavelets, if such filters satisfy those conditions along with the conditions of orthogonality and the MR axioms. The succeeding sections consider this problem.

3.2 Generalised Multi-resolution Axioms.

The Generalised Multi-resolution analysis(GMRA) is an extension of the conventional MRA[17] . The new set of multi-resolution axioms are as under.

Definition 3.2.1 *A Generalised Multi-resolution analysis of* $L^2(\Re)$ *is a sequence of closed subspaces* $\ldots, v_{-1}, v_0, v_1, v_2, \ldots$ *such that*

(M1) $v_n \subset \bigcup_{j=1}^{N} v_{n-j}$
(M2) $\bigcup_{n=-\infty}^{\infty} v_n$ *is dense in* $L^2(\Re)$ *and* $\bigcap_{n=-\infty}^{\infty} v_n = 0$
(M3) $f(x) \in v_n \iff f(2x) \in v_{n-1}$
(M4) $f(x) \in v_0 \iff f(x-k) \in v_0$ *for all* k *element* Z
(M5) There exists an isomorphism $\mathbf{I}$ *from* v_0 *onto* $\ell^2(Z)$ *which commutes with the action of* Z

The only difference of this Generalised MRA as compared to the conventional MRA is in (M1). In (M5) the action of Z over v_0 is the translation of functions by integers whereas the action of Z over $\ell^2(Z)$ is the usual translation. The approximation of a function $f(x)$ at resolution 2^j is the orthogonal projection of $f(x)$ on V_j where

$$V_n \triangleq \bigcup_{j=1}^{N} v_{n-j} \tag{3.1}$$

N is referred to be the order of the MRA. The conventional MRA becomes a special case of Generalised MRA when $N = 1$

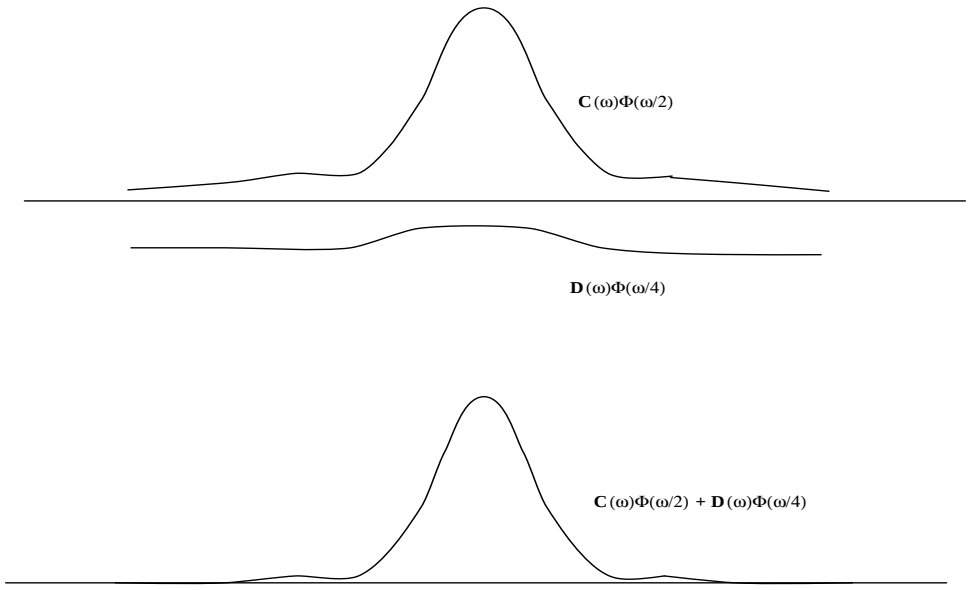

Figure 3.1: Motivation for Generalised MRA.

3.3 Orthogonal basis of multi-resolution analysis.

The operator Z is as defined in chapter 2.Now the natural question arises whether we can have a orthonormal basis for the above Generalised Multi-resolution spaces. The following theorem [9] gives the existence of an orthonormal basis functions and represents them in terms of the basis functions $g(x-k)$.

Theorem 3.3.1 *Let $v_0 \subset L^2(\Re)$ and let $g \in v_0$ be such that (M4)-(M5) hold.*
(a). If $\phi \in L^2(\Re)$ is defined as

$$\hat{\phi}(\epsilon) = \frac{\hat{g}(\epsilon)}{\Gamma(\epsilon)} \quad , \text{ where} \tag{3.2}$$

$$\Gamma(\epsilon) = (\sum_{k=-\infty}^{\infty} \mid \hat{g}(\epsilon + 2k\pi) \mid^2)^{\frac{1}{2}} \tag{3.3}$$

Then the functions $\phi(.-k)$ form an orthonormal basis of v_0.
(b). If $\sigma \in L^\infty(\Re)$ is a 2π periodic function with $|\sigma(\epsilon)| = 1 a.e.$, and if θ is defined as $\hat{\theta}(\epsilon) = \sigma(\epsilon).\hat{\phi}(\epsilon)$, then $\theta \in v_0$ and $\theta(.-k), k \in Z$ is an orthogonal basis of v_0

Conversely if $\theta \in v_0$ is such that $\| \theta \| = 1$ and the functions $\theta(.-k), k \in Z$ is an orthonormal basis of v_0 and $\hat{\theta}(\epsilon) = \sigma(\epsilon)\hat{\phi}(\epsilon)$ where $\sigma \in L^\infty(\Re)$ is a 2π periodic function with $\mid \sigma(\epsilon) \mid = 1 a.e.$

(c). Let $\phi \in v_0$ be such that the system $\phi(. - k), k \in Z$, is orthonormal, then

$$\sum_{k=-\infty}^{\infty} \mid \hat{\phi}(\epsilon + 2k\pi) \mid^2 = 1 \, a.e. \tag{3.4}$$

This theorem gives an infinite set of orthonormal basis functions of v_0 satisfying M4 and M5 depending on the choice of $\sigma(\epsilon)$.

3.4 Construction of the Scaling function

Theorem(3.3.1) gives a means of finding out the orthonormal basis functions provided we have a multi-resolution space, which satisfies the multi-resolution axioms. But practically, we find out a multi-resolution space, by the choice of the orthonormal basis functions. The properties of the multi-resolution decomposition depends on the choice of these functions.

For simplicity of analysis, in this work, the order of the MRA is restricted to N=2.

Once the functions are chosen, the spaces v_n are defined as the span of the functions $a_n\phi(2^n. - k)$, where a_n are some constants chosen for normalisation. So the problem of finding out a MRA simplifies into the choice of the orthonormal basis functions so that the spaces v_n satisfies (M1) - (M5).

As we assumed orthogonality of ϕ with respect to the translates, we have

$$< a_n\phi(2^n x - k), a_n\phi(2^n x - l) >= \delta(k, l) \tag{3.5}$$

where $< ., . >$ represents the inner product of the two argument functions.

From the above equation, the constant a_n turns out to be $2^{\frac{n}{2}}$. Hence the orthonormal basis vectors of v_n are $2^{\frac{n}{2}}\phi(2^n. - k), k \in Z$

Here after for ease of representation, we will use the following notation as $f(j,k)(x) = 2^{\frac{j}{2}}.f(2^j x - k)$. According to the notation, the orthonormal basis vectors of v_n are $\{\phi(n,k)(x), k \in Z\}$.

Assume that $v_n, n \in Z$ defines a generalised multi-resolution analysis of $L^2(\Re)$ generated by the basis function ϕ, and that $\{\phi(. - k) \mid k \in Z\}$ is an orthonormal

family. The function $\phi(x)$ lies in v_0 and hence in $v_1 \bigcup v_2$ due to (M1). Hence we can find sequences $(c_k, d_k, k \in Z)$ such that

$$\phi(x) = \sqrt{2}. \sum_{k=-\infty}^{\infty} c_k.\phi(2x-k) + 2. \sum_{l=-\infty}^{\infty} d_l.\phi(4x-l) \tag{3.6}$$

Taking the Fourier Transform of both the sides we get

$$\hat{\phi}(\omega) = C(\frac{\omega}{2}).\hat{\phi}(\frac{\omega}{2}) + D(\frac{\omega}{4}).\hat{\phi}(\frac{\omega}{4}) \tag{3.7}$$

where $C(\omega)$ and $D(\omega)$ are given by

$$C(\omega) = \frac{1}{\sqrt{2}} \sum_{k=-\infty}^{\infty} c_k \exp(j\omega k) \tag{3.8}$$

$$D(\omega) = \frac{1}{2} \sum_{l=-\infty}^{\infty} d_l \exp(j\omega l) \tag{3.9}$$

As the ϕ satisfies (3.6), which relates ϕ to the dilates of itself(scales) we call it as the scaling function.

Equation (3.6) gives the constraint, to be satisfied by the orthogonal basis function $\phi(x)$, so that the spaces spanned by $2^{\frac{n}{2}}\phi(2^j x - k)$ satisfy (M1). For the spaces to satisfy (M2) we need to have $\lim_{j\to-\infty} T_j(f) \equiv f$ for every function $f \in L^2(\Re)$, where T_j is the projection operator to the space v_j. The following theorem [17] gives the condition under which this condition holds.

Theorem 3.4.1 *Let g be a regular function and let the kernel K be given by $K(x,y) = \sum_{k=-\infty}^{\infty} g(x-k)\overline{g}(y-k)$ Let $T_\lambda : L^2(\Re) \to L^2(\Re)$ be the integral operator*

$$(T_\lambda f)(x) = \lambda \int K(\lambda x, \lambda y) f(y) dy$$

Then the following assertions are equivalent

$$\begin{array}{lll} (1). & \lim_{\lambda\to\infty} \parallel T_\lambda f - f \parallel_2 = 0, & \forall f \in L^2(\Re) \\ (2). & \int K(x,y)dy = 1 & \forall x \in \Re \end{array}$$

Applying the above theorem to the scaling function, assuming regularity, so that the

spaces satisfy (M2), we get

$$\sum_{k=-\infty}^{\infty} \phi(x-k) \int_{\Re} \overline{\phi}(y-k)dy = \overline{\hat{\phi}}(0). \sum_{k=-\infty}^{\infty} \phi(x-k) = 1$$

Integrating this expression over $[0,1]$ we get,

$$\mid \hat{\phi(0)} \mid^2 = 1 \tag{3.10}$$

Once we assume that v_n is generated by $(2^{\frac{n}{2}}\phi(2^n x - k), k \in Z)$, which is regular and satisfies (3.6), (3.5) & (3.10), the spaces $(v_n, n \in Z)$ give a Generalised Multi-resolution decomposition of $L^2(\Re)$. The MR axioms (M3),(M4) and (M5) will be automatically satisfied.

As mentioned before, the properties of the MRA will depend on the scaling function chosen, satisfying the conditions above. Hence the choice of the MRA boils down to the choice of the coefficients ($c_k \; and \; d_k, k \in Z$). We will now derive the conditions the coefficients has to satisfy so that the scaling function will satisfy the above conditions(GMR Axioms along with the orthogonality constraint).

Equation(3.6) can be re-written as given below for simplification.

$$\phi(x) = \eta(x) + \gamma(x) \quad \text{where} \tag{3.11}$$

$$\eta(x) = 2. \sum_{k=-\infty}^{\infty} d_k \phi(4x-k) \quad \text{and} \tag{3.12}$$

$$\gamma(x) = \sqrt{2}. \sum_{k=-\infty}^{\infty} c_k \phi(2x-k) \tag{3.13}$$

As mentioned before $\{\phi(j,k)(x), k \in Z\}$ are the basis functions of v_j. We define two new sequences of spaces $(u_j \& w_j, j \in Z)$, where

$$u_j \equiv span\{\eta(j-2,k)(x)\} \tag{3.14}$$

$$w_j \equiv span\{\gamma(j-1,k)(x)\} \tag{3.15}$$

This implies that u_j and w_j are the subspaces of v_j due to equations (3.12) and (3.13) as shown in figure(3.5).

As a special case we will consider the case where u_j and v_j are orthogonal to each other, $\forall j \in Z$. This assumption will greatly simplify the following analysis. This assumption imposes a constraint on the coefficients ($c_k \; and \; d_k, k \in Z$). This constraint

is derived in Appendix A to be

$$D(\omega) = \alpha(\omega)\overline{C}(\omega + \pi) \tag{3.16}$$

where $\alpha(\omega)$ is a π periodic function.

We can now see the constraint imposed by the orthogonality constraint given by equation (3.5), on the coefficients c_k's and d_k's. Equation (3.5) implies that,

$$< \phi(x-k), \phi(x-l) >= \delta(k,l) \tag{3.17}$$

Substituting from equation (3.6) we get

$$\begin{aligned}
\sum_m \sum_o c_m c_o < \phi(2x-2k-m), \phi(2x-2l-o) > \quad &+ \\
\sum_n \sum_p d_n d_p < \phi(4x-4k-n), \phi(4x-4l-p) > \quad &+ \\
\sum_m \sum_p c_m d_p < \phi(2x-2k-m), \phi(4x-4l-p) > \quad &+ \\
\sum_0 \sum_n c_o d_n < \phi(2x-2l-o), \phi(4x-4k-n) > \quad &= \delta(k,l)
\end{aligned} \tag{3.18}$$

In the above equation, the last two terms are the cross terms. it is shown in the Appendix A that they vanish if equation (3.16) are satisfied and

$$C(\omega) = -C(\omega + \pi), \forall \omega \tag{3.19}$$

So when equation (3.16) and equation (3.19) is satisfied, equation (3.18) simplifies to

$$\begin{aligned}
\sum_m \sum_o c_m c_o < \phi(2x-2k-m), \phi(2x-2l-o) > \quad &+ \\
\sum_n \sum_p d_n d_p < \phi(4x-4k-n), \phi(4x-4l-p) > \quad &= \quad \delta(k,l)
\end{aligned} \tag{3.20}$$

It is shown in Appendix A that in the Fourier domain equation(3.20) reduces to

$$\begin{aligned}
|C(\frac{\omega}{2})|^2 + |C(\frac{\omega}{2}+\pi)|^2 + |D(\frac{\omega}{4})|^2 + |D(\frac{\omega}{4}+\frac{\pi}{2})|^2 + \\
|D(\frac{\omega}{4}+\pi)|^2 + |D(\frac{\omega}{4}+\frac{3\pi}{2})|^2 = 1
\end{aligned}$$

Substituting from (3.16) in the above equation we get

$$|C(\frac{\omega}{2})|^2 + |C(\frac{\omega}{2}+\pi)|^2 + |\alpha(\frac{\omega}{4})|^2[|C(\frac{\omega}{4})|^2 + |C(\frac{\omega}{4}+\pi|^2] \\ +|\alpha(\frac{\omega}{4}+\frac{\pi}{2})|^2[|C(\frac{\omega}{4}+\frac{\pi}{2})|^2 + |C(\frac{\omega}{4}+\frac{3\pi}{2}|^2] = 1 \tag{3.21}$$

The above constraint is a coupled one and to find a set of filters that satisfy the above constraint is difficult. We split the above constraint to two constraints such that the filter transfer functions can be found out easily. They are as under

$$|C(\omega)|^2 + |C(\omega+\pi)|^2 = k_1 \tag{3.22}$$

$$|\alpha(\omega)|^2 + |\alpha(\omega+\frac{\pi}{2})|^2 = k_2 \text{ and as eqn(3.21) is to be satisfied} \tag{3.23}$$

$$k_2 = \frac{1}{2k_1} - \frac{1}{2} \tag{3.24}$$

If we choose $k_1 = 1$, then the filters correspond to the ordinary uni-wavelet case. We make an arbitrary choice of $k_1 = \frac{1}{2}$ & $k_2 = \frac{1}{2}$.

The constraints (3.22), (3.23), (3.19) & (3.16) are the sufficient conditions for the solution of the two-scale relationship to satisfy the MR axioms M1, M3, M4 & M5 along with the orthogonality constraint (3.5).

Equation (3.10) is the sufficient condition for M2 to be satisfied and it will be satisfied if $\hat{\phi}(\omega) = 1$. This implies

$$C(0) + D(0) = 1$$

$$\Rightarrow \quad C(0) + \alpha(0)C(\pi) = 1 \tag{3.25}$$

By equation (3.22) we have

$$|C(0)|^2 + |C(\pi)|^2 = \frac{1}{2} \tag{3.26}$$

By the constraint (3.19) this reduces to

$$C(0) = \pm\frac{1}{2}$$

From the above constraints it is clear that the only feasible solution is

$$C(0) = -C(\pi) = \tfrac{1}{2} \tag{3.27}$$

$$\alpha(0) = -1, \alpha(\frac{\pi}{2}) = 0 \tag{3.28}$$

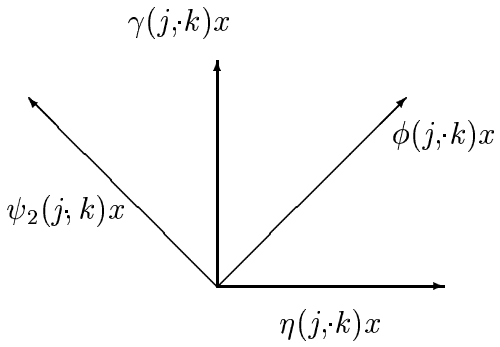

Figure 3.2: The basis vectors of the decomposition

So the constraints the coefficients have to satisfy, for the solution to satisfy the MR axioms and orthogonality condition are,

$$|C(\omega)| = \frac{1}{2} \tag{3.29}$$

$$\arg(C(\omega)) = -\arg(C(\omega+\pi)) \tag{3.30}$$

$$D(\omega) = \alpha(\omega)\overline{C}(\omega+\pi) \tag{3.31}$$

$$|\alpha(\omega)|^2 + |\alpha(\omega+\frac{\pi}{2})|^2 = 1 \tag{3.32}$$

$$\alpha(\omega) = \alpha(\omega+\pi) \tag{3.33}$$

$$C(0) = -C(\pi) = \frac{1}{2} \tag{3.34}$$

$$\alpha(0) = 1, \alpha(\frac{\pi}{2}) = 0 \tag{3.35}$$

From the above equations it is clear that the filter $C(\omega)$ reduces to a simple all pass filter with the constraint (3.30) and (3.34).

As $\alpha(\omega)$ is π periodic, we can represent it as

$$\alpha(z) = \beta(z^2), \text{with} \tag{3.36}$$

$$|\beta(\omega)|^2 + |\beta(\omega+\pi)|^2 = 1 \tag{3.37}$$

It can be realised as in figure(2.5).

3.5 Construction of the Wavelet basis

As we move from a higher resolution to a lower resolution, we lose some information. This lost information can be extracted as orthogonal projection to some space. The lost information basically comprises of two parts:

(1) Subspace of v_j which is not present in $u_j \& w_j$. We call this space $O1_j$ and assume it to be spanned by $\psi_1(j,k)(x)$.

(2) The basis vectors of u_j and w_j are given by (3.14) and (3.15) respectively. The basis vectors of v_j is obtained by adding the corresponding basis vectors of w_{j-1} and u_{j-2}, *i.e.* $\gamma(j-1,k)(x)$ and $\eta(j-2,k)$. Hence when we move from the space $w_{j-1} \bigoplus u_{j-2}$ to v_j , we are taking the orthogonal projection onto v_j. So the lost information is given by the projection to the orthogonal compliment space of v_j in $w_{j-1} \bigoplus u_{j-2}$. We can call that space as $O2_j$

As can be seen from the figure below $O2_j$ is spanned by $\psi_2(j,k)(x)$ where

$$\psi_2(j,k)(x) = \gamma(j,k)(x) - \eta(j,k)(x) \tag{3.38}$$

Now we have to express $\psi_1(j,k)(x)$ in terms of the dilates and translates of ϕ's.

From equation (3.12) we have

$$\hat{\eta}(4\omega) = D(\omega).\hat{\phi}(\omega)$$

and by equation (3.31) we have

$$\hat{\eta}(4\omega) = \alpha(\omega)\overline{C(\omega+\pi)}.\hat{\phi}(\omega)$$

Now consider the function

$$\hat{\theta}(2\omega) = \overline{C(\omega+\pi)}.\hat{\phi}(\omega)$$

According to [9] the space spanned by the functions $\theta(j-1,k)(x)$ will span the orthogonal compliment space of w_j in v_j. We can call this space as t_j, see figure(3.5) . From this orthogonal compliment space t_j, we extract the space u_j spanned by $\eta(j-2,k)(x)$, where

$$\hat{\eta}(2\omega) = \beta(\omega)\hat{\theta}(\omega)$$

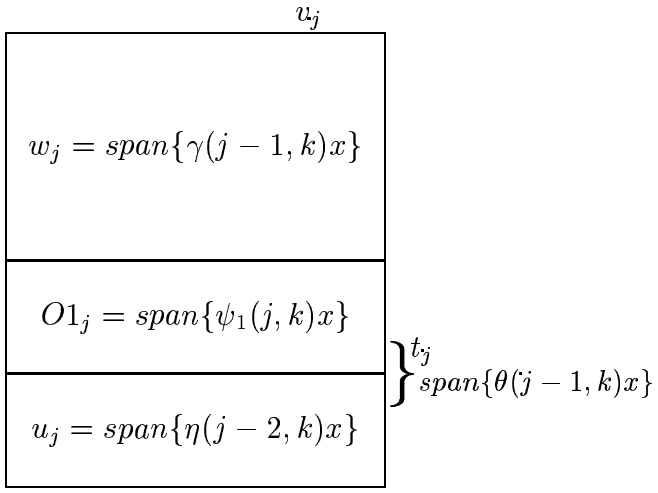

Figure 3.3: The decomposition of the space v_j

whose orthogonal compliment space is spanned by the set of functions $\psi_1(j-2,k)(x)$ where

$$\hat{\psi_1}(2\omega) = \overline{\beta(\omega+\pi)}\hat{\theta}(\omega)$$

Hence we have,

$$\hat{\psi_1}(4\omega) = \overline{\alpha(\omega+\frac{\pi}{2})C(\omega+\pi)}.\hat{\phi}(\omega) \tag{3.39}$$

For convenience this can be written as

$$\hat{\psi_1}(4\omega) = E(\omega)\hat{\phi}(\omega) \quad \text{where,} \tag{3.40}$$

$$E(\omega) = \overline{\alpha(\omega+\tfrac{\pi}{2})C(\omega+\pi)} \tag{3.41}$$

Combining equation (3.38) and (3.39) in the matrix form we have

$$|\hat{\Psi}(2\omega)| = \begin{vmatrix} 0 & E(\frac{\omega}{2}) \\ C(\omega) & -D(\frac{\omega}{2}) \end{vmatrix} |\hat{\Phi}(2\omega)|, \quad \text{where} \tag{3.42}$$

$$\hat{\Psi}(\omega) = \left| \begin{array}{c} \hat{\psi}_1(\omega) \\ \hat{\psi}_2(\omega) \end{array} \right| \quad \text{and} \tag{3.43}$$

$$\hat{\Phi}(\omega) = \left| \begin{array}{c} \hat{\phi}(\frac{\omega}{2}) \\ \hat{\phi}(\omega) \end{array} \right| \tag{3.44}$$

The multi-scale relationship can also be represented in the matrix form as

$$|\hat{\Phi}(2\omega)| = \left| \begin{array}{cc} C(\omega) & D(\frac{\omega}{2}) \\ 1 & 0 \end{array} \right| |\hat{\Phi}(\omega)| \tag{3.45}$$

Equations (3.42) and (3.45) imply that the Generalised Multi-resolution Decomposition is a special case of the multi-wavelet decomposition. Although we started with the case where a particular resolution space is spanned by the translates of the scaling function dilated to two different scales, there exists an equivalent orthogonal multi-wavelet, which gives the same decomposition as in the above case. Such a multi-wavelet has $\eta(j-1,k)(x)$ and $\phi(j,k)(x)$ as the orthogonal multi-scaling functions.

3.6 Wavelet expansion and Filtering

In the Multi-resolution decomposition, we decompose the signal to different resolutions, by projecting it to the space spanned by the wavelet vectors $\psi_1(j,k)$ and $\psi_1(j,k)$ for different values of j and k. The amount of computation required for this can be greatly reduced , if a method similar to Mallat's algorithm is used . The algorithm to achieve this is derived in this section.

We assume certain notations in this section for ease of representation. They are stated below .

$$\begin{aligned} a_k^n(f) &= < f, \phi(n,k) > \\ b1_k^n(f) &= < f, \psi_1(n,k) > \\ b2_k^n(f) &= < f, \psi_2(n,k) > \end{aligned}$$

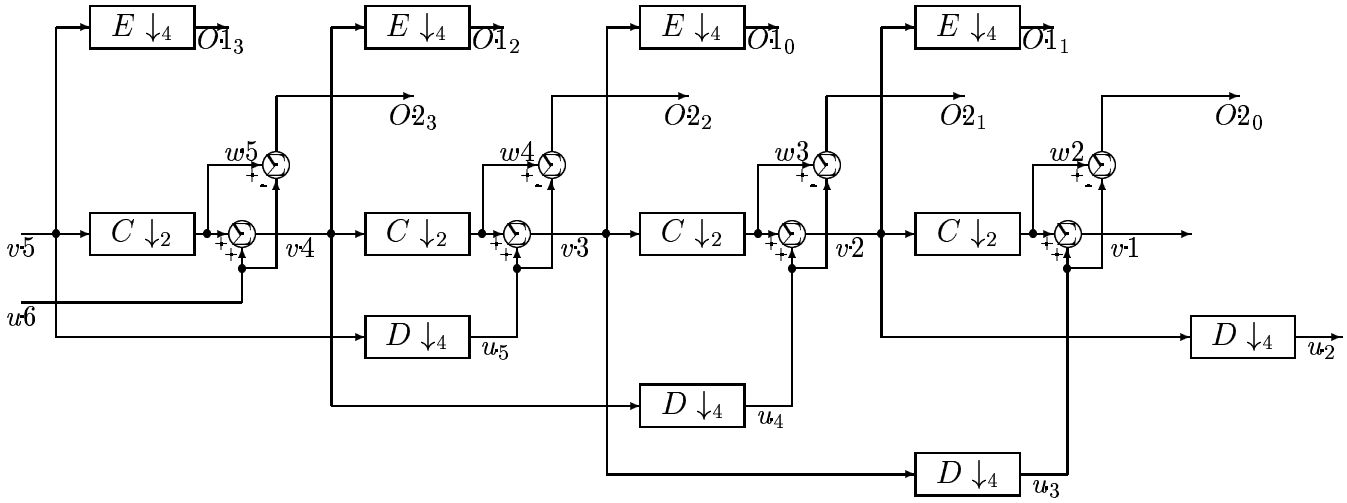

Figure 3.4: Implementation of Generalised Multi-resolution Decomposition.

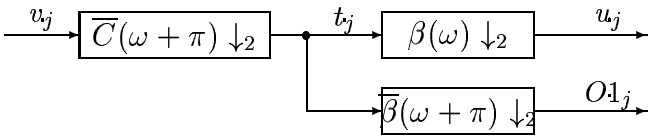

Figure 3.5: Implementation of the filters $D(\omega)$ and $E(\omega)$

The projection operators to different spaces are given as

$$\begin{aligned} P_n(f) &= \sum_{k=-\infty}^{\infty} a_k^n(f)\phi(n,k) \\ Q1_n(f) &= \sum_{k=-\infty}^{\infty} b1_k^n(f)\psi_1(n,k) \\ Q2_n(f) &= \sum_{k=-\infty}^{\infty} b2_k^n(f)\psi_2(n,k) \end{aligned}$$

As given by (M1), $v_{n-2} \subset v_{n-1} \bigcup v_n$. Hence if we know $P_n(f)$ and $P_{n-1}(f)$ we can find out $P_{n-2}(f)$ in terms of the the previous functions.

$$c_k^{n-2} =< f, \phi(n-2,k) >$$

Expanding the previous equation by substituting for $\phi(n-2,k)$ in terms of $\phi(n-1,.)$ and $\phi(n,.)$, we get

$$\begin{aligned} a_k^{n-2} &= \textstyle\sum_{l=-\infty}^{\infty} c_l < f, \phi(n-1,2k+l) > + \\ & \textstyle\sum_{m=-\infty}^{\infty} d_m < f, \phi(n,4k+m) >, \quad \text{which is simplified as} \end{aligned}$$

$$a_k^{n-2} = \sum_{l=-\infty}^{\infty} c_{-l} a_{2k-l}^{n-1} + \sum_{m=-\infty}^{\infty} d_{-m} a_{4k-m}^{n}$$

This can be seen as

$$a^{n-2} = \quad (\tilde{c} * a^{n-1}) \downarrow_2 + \quad (\tilde{d} * a^n) \downarrow_4 \tag{3.46}$$

where '*' denotes convolution of the two sequences and $\downarrow_M$ denotes down-sampling by a factor M. $\tilde{c}$ denotes the sequence c_{-l} and a^{n-1} denotes the sequence a_l^{n-1}

Similarly it can be seen that

$$d1^{n-2} = \quad (\tilde{e} * a^n) \downarrow_4 \tag{3.47}$$

$$d2^{n-2} = \quad (\tilde{c} * a^{n-1}) \downarrow_2 - \quad (\tilde{d} * a^n) \downarrow_4 \tag{3.48}$$

The Generalised Multi-Resolution decomposition is as given in Figure(2.4).

3.7 The Approximation order of the Generalised MRA

As mentioned in Chapter 2, the approximation order of an MRA refers to the degree of the highest degree polynomial that can be exactly represented by the translates of the scaling functions. The asymptotic accuracy of the approximation is decided by the approximation order.

As it is seen from the above sections that the Generalised MRA is a special case of the multi-wavelet MRA, we can borrow the results available on the approximation order from the multi-wavelet theory. We consider the analysis of the equivalent orthogonal multi-wavelet formed by $\eta(j-1,k)(x)$ and $\phi(j,k)(x)$ as mentioned above as the approximation order of the equivalent system is the same as that of the Generalised MRA. From equations (2.28), for $j=0$ we have,

$$u.M(0) = u, \text{ and,} \tag{3.49}$$

$$u.M(\pi) = 0. \tag{3.50}$$

where u is an some arbitrary vector. For the above mentioned equivalent orthogonal multi-wavelet

$$M(\omega) = \begin{vmatrix} C(\omega) & \beta(\omega) \\ C(\omega+\pi) & 0 \end{vmatrix} \tag{3.51}$$

Substituting in the conditions (3.49) and (3.50), we get

$$\beta(\pi) = 0 \tag{3.52}$$

$$C(0) = \frac{1}{1-\beta(0)^2} \tag{3.53}$$

$$C(\pi) = \frac{-\beta(0)}{1-\beta(0)^2} \tag{3.54}$$

It can be easily seen that the only class of solutions that satisfy the orthogonality constraints in equation(3.22) and equation(3.23), and has an approximation order of one is the class of uni-wavelets. The orthogonal Generalised MRA fails to have high approximation orders as the filters $C(\omega)$ and $D(\omega)$ are respectively all-pass and low-pass contrary to he expectation that they are respectively low-pass and high-pass. It is the orthogonality constraint that made it impossible for the wavelets to have a high

approximation order.

It can be quiet easily shown that the biorthogonal class, has a high approximation order, with possibly a shorter support as compared to the uni wavelets. But the more general class, the class of multi wavelets have wavelets that exhibit all the above properties simultaneously.

3.8 Conclusion

In this chapter, a possible extension to the conventional Multi-Resolution analysis was explored. The aim was to look for wavelets that have all the four desired properties - orthogonality, short support, symmetry and high approximation orders.

It was found that the class of Orthogonal Generalised MRA wavelets do not have even first order approximation property that is present in all uni-wavelets. This is because the orthogonality constraint has over-constrained the filters to behave in the desired manner. It is true that the bi-orthogonal GMRA wavelets do have high approximation orders. As the GMRA orthogonal wavelets are very irregular , they might be better to deal with irregular signals where the localisation in frequency is minimal.

It was also found that the class of GMRA wavelets forms a subclass of the Multi-wavelets. The class of multi-wavelets have elements that have all the desired conditions simultaneously.

Chapter 4

Wavelet Transform Coding of Collage Error

4.1 Introduction

Conventional Fractal Image coding, as described below, finds an optimal domain block for each range block, so that the error in the representation of the range block is minimised. Later this scheme was modified by Munro et al [4] , who represented the residual error in the above mentioned representation using piecewise polynomial functions, and estimated the parameters of the transform (contraction factor and parameters of the polynomials) so that the MSE is minimised. This scheme is termed as Bath Fractal transform(BFT).

In this chapter we suggest a scheme in which the residual errors are represented in a compact fashion in a transform domain. In this domain, different features of the error signal with different perceptual implications get separated into different bands, so that we can encode the error to yield a decoded image of a better perceptual quality. This scheme also gives a more graceful degradation in performance as the compression ratio is increased.

The remainder of this chapter is organised as follows. In the next section we present a brief review of Fractal Image compression scheme and BFT. In the third section an alternate interpretation of BFT is mentioned . The fourth section gives a justification of the choice of the particular transform in the encoding of the error, the fifth section describes the method and the last section gives the results.

4.2 Fractal Image Compression

We present a brief review of the mathematical foundations of Fractal Image Compression in this section. For a detailed treatment refer [6].

In conventional Fractal Image compression, a given image is approximated as the attractor of a contractive mapping. The definition of the contractive mapping, and the uniqueness of its attractor are given below .

Definition 4.2.1 *A sequence of points* $\{x_n\}$ *in a metric space is called a* **Cauchy sequence** *if for every* $\epsilon > 0$ *there exists an integer* N *such that*

$$d(x_m, x_n) < \epsilon, \quad \forall n, m > N \tag{4.1}$$

In the above definition $d(x, y)$ denotes the distance between the two elements x and y, where x and y are the elements of the metric space.

Definition 4.2.2 *A metric space* χ *is said to be complete if every Cauchy sequence in* χ *converges to a limit point in* χ.

Definition 4.2.3 *Let* (χ, d) *denote a metric space. A map* $w : \chi \to \chi$ *is* **Lipschitz** *with a Lipschitz factor* s *if there exists a positive real number* s *such that*

$$d\left(w(A), w(B)\right) \leq sd\left(A, B\right), \quad \forall A, B \in \chi \tag{4.2}$$

If the Lipschitz factor $s < 1$, then w is said to be a **contractive mapping** with a contractivity s. The theorem given below, gives the uniqueness of the fixed point of a contractive mapping.

Theorem 4.2.1 *(***The Contraction Mapping Fixed Point Theorem***)*
Let χ *be a complete metric space and* $w : \chi \to \chi$ *be a contractive mapping. Then there exists a unique fixed point* $F \in \chi$ *such that for any point* $P \in \chi$

$$F = w(F) = \lim_{n \to \infty} w^{on}(P). \tag{4.3}$$

Such a point is called the **fixed point** *or the* **attractor** *of* w.

Definition 4.2.4 *A collection* $w_1, w_2, \ldots, w_n$ *of contractive maps on a metric space* (χ, d) *is called an iterated function system(IFS).*

Using the above concepts, we can see how an IFS can be used for the encoding of images. Consider an image signal given by $G \in \chi$. Further let

$$\hat{G} = W(\hat{G}) = \lim_{n \to \infty} W^{on}(P), \quad \forall P \in \chi \tag{4.4}$$

where W is a contractive transformation, and $d(G, \hat{G})$ is small. If we can determine a "W" such that the error given by $d(G, \hat{G})$ is within some acceptable limits, and if the contractive mapping W can be represented using fewer bits as compared to the representation of G, then we achieve compression.

Unfortunately, these theorems do not provide us with a method of arriving at the map w. This problem is simplified to a large extent by collage theorem.

Theorem 4.2.2 Collage Theorem *Let (χ, d) be a metric space and $W : \chi \to \chi$ be a contractive mapping with a contractivity s. Let $\hat{G}$ be the fixed point of W. Then,*

$$d(G, \hat{G}) \leq \frac{1}{1-s} d\left(G, W(G)\right). \tag{4.5}$$

The above theorem gives an upper bound of the error in terms of the distance between the actual image G and $W(G)$. The above theorem implies that the error can be minimised if $d(G, W(G))$ is minimised. Hence the problem of finding the fractal code W for the image G can be restated as follows:

Find W such that $d(G, w(G))$ is minimised.

For simplicity, W is assumed to be of the form

$$W = \bigcup_{i=1}^{N} w_i, \tag{4.6}$$

where each w_i is a contractive mapping. Now we can see a way of defining w_i. Let us assume that the region of support of the image is the unit square $I_M^2 = [0, M]\text{x}[0, M]$, and the dynamic range of the grey level of the image is scaled to the interval $I = [0, 1]$. Then the parametric form of the transformations $w_i : I_M^2 \text{x} I \to I_M^2 \text{x} I, i = 1, \ldots, N$ is chosen as

$$w_i \begin{pmatrix} x \\ y \\ z \end{pmatrix} = \begin{pmatrix} a_i & b_i & 0 \\ c_i & d_i & 0 \\ 0 & 0 & s_i \end{pmatrix} \begin{pmatrix} x \\ y \\ z \end{pmatrix} + \begin{pmatrix} e_i \\ f_i \\ o_i \end{pmatrix}, \tag{4.7}$$

where (x, y) denotes the coordinates of a point in I_M^2 and $z = g(x, y)$ denotes the

intensity or grey level at (x, y). Associated with each w_i is a range block $R_i \in I_M^2$ and a domain block $D_i \in I_M^2$. The encoding scheme can be described as below.

- Divide the image into non-overlapping range blocks.
- Find the optimal domain block for each range block such that distance between the range block and the one represented by the contractive mapping is minimised.

The so chosen optimal domain block for a range block, and the parameters obtained, represents the IFS.

It is to be noted that in equation(4.7), a constant grey level is o_i added. This can be extended to some parametric function in x & y so that the error in approximation is minimised. In this case the number of parameters is increased. In the case where the parametric function is a piecewise polynomial in x & y we get the BFT.

4.3 An alternate interpretation of the BFT

In BFT we approximate the image $G \in B(I_M)$ (Banach space of functions in the interval [0, M] x [0, M]) as $\hat{G}$, the solution of a Self affine system given by

$$\hat{G} = \bigcup_{i=[0,0]}^{[M,M]} w_i(S_{n_i} \circ \hat{G}) \tag{4.8}$$

Here S_{n_i} is the *block get operator*, which selects a block in the interval $[n_i, n_i + [1, 1]]$ and translates it to the interval I([0, 1] x [0, 1]). $\hat{G}$ is the attractor of the IFS defined by $\{w_i\}$, where w_i is defined as

$$\begin{aligned} w_i(x, y) &= (u_i(x), v_i(x, y)), \quad where \\ u_i(x) &= \frac{(x + i)}{N}, \quad and \\ v_i(x, y) &= \lambda_i(x) + s_i.y \end{aligned}$$

It should be noted that the variables i, j, x are vectors of dimension 2. For the above mapping to be a contractive mapping $|s_i| < 1, \forall i$. For each i, the parameters n_i and s_i are chosen so that the mean square error of the approximation is minimised.

In BFT, the polynomial $\lambda(x)$ is a first order polynomial of its arguments. It should be noted that the above representation becomes an approximation only when

the $\lambda(x)$ is constrained to be an element of some finite dimensional space, as in the case of BFT.

For the time being we will consider $\lambda_i(x)$ to be elements of $B(I)$, and for ease of representation we call the direct product $(\lambda_{00}(x), \lambda_{01}(x), \ldots, \lambda_{MM}(x))$ as $\lambda \in B = \bigotimes_j B(I)$. Also we set $S = (s_{00}, s_{01}, \ldots, s_{MM})$ and $N = (n_{00}, n_{01}, \ldots, n_{MM})$. Let the attractor , defined by a particular choice of the parameters(N and S) be called as $f_\lambda$to denote the dependence on λ. We state a theorem, which for conventional fractal interpolation functions is proved in [15]

Theorem 4.3.1 *The mapping $\lambda \xrightarrow{\theta} f_\lambda$ is a linear isomorphism from B to $B(I_M)$.*

The proof can be obtained by following along the same lines as that of the theorem in [15].

It is to be noted that the isomorphism is dependent on the choice of the parameters N and S. So the parameter estimation in BFT can be seen as choosing the optimal isomorphism so that the projection of λ onto the finite dimensional space(piecewise polynomial space) is maximised. The parameter vector S can be estimated using a closed form expression, while the parameter vector N can be estimated only using a search in the entire parameter space.

In BFT, λ is represented by the projection to the piecewise polynomial space, and hence the number of parameters used for the representation of λ remains a constant irrespective of the amount of detail available at each section. It would be better if we can reduce the number of parameters at smooth areas and provide more parameters where there is more detail. This can be solved using adaptive subdivision, where we solve the parameters again for smaller block sizes in region where the error is more, but the computation complexity involved is more.

It is seen that transform techniques are very effective in coding of image information. The question is whether we can use some transform technique to code the collage error signal (λ). The next section discusses this issue.

4.4 Choice of the Transform

The Error signal(λ) has two significant features which will help us to decide on the transform to be used.

- The error signal is discontinuous at the block boundaries. These discontinuities if not represented will result in blockiness in the reconstructed image.
- The fractal encoding technique fails to capture the fine details of the image. This contains the edge details of the image also.

The perceptual degradation of the reconstructed image due to the above features not being represented, is different in both the cases. The blockiness of the reconstructed image is a very disturbing feature, while the loss of fine details are not as disturbing. The fine details themselves can be classified into details at different scales(eg. loss of the edge details of the face of the Lena image is more disturbing than the loss of the details of the texture of the hat).

The presence of edge details at different scales in the collage error signal, suggest the use of a multi-resolution representation of the error. This multi-resolution representation should separate out the above mentioned features to different scales so that the features which cause the least perceptual disturbance can be attenuated.

It can be seen that the discontinuities that occur at the block boundaries are abrupt discontinuities where the Lipschitz regularity parameter "α" is zero. These discontinuities will cause the continuous wavelet transform to have a significant magnitude at all scales, as shown below, whereas smooth signals (where the Lipschitz exponent > 0) will cause the CWT to decay exponentially.

In the approximation of the edges, it is better to consider the maximum error(sup norm), rather than the mean squared error. So to have an estimate of the decay of the maximum error, we consider the analysis wavelet at the scale $'s'$ as,

$$\psi_s(x) = \frac{1}{s}\psi(\frac{x}{s}) \tag{4.9}$$

Suppose we have a step function at x=a, given by $f(x) = U(x-a)$. We have to compute the continuous wavelet transform of this function at x=a. By the definition of the continuous wavelet transform, the CWT of the step function is

$$W_c f(x,s) \;=\; f * \psi_s(x) \;=\; \frac{1}{s}\int_a^{\infty} \psi\left(\frac{x-y}{s}\right) dy \tag{4.10}$$

It can be shown with some algebraic manipulation that

$$W_c f(x,s) \;=\; \psi_s^1(x-a), \quad \text{where} \tag{4.11}$$

$$\psi_s^1(x) = \int_{-\infty}^{\frac{x}{s}} \psi(y)dy \tag{4.12}$$

Equation (4.11) implies that the peak magnitude of the continuous wavelet transform coefficient is a constant, irrespective of the scale. This is because the peak magnitude of the function $\psi_s^1(x)$ is the same irrespective of s which is implied from equation(4.12) . The constant magnitude of the CWT implies that the absolute magnitude of the error caused by the truncation of the wavelet coefficients at a higher scales, decays only linearly as $s \to 0$.

But if careful choice of the wavelet is made, the Discrete wavelet coefficients corresponding to the edge at $x = a$ can be made to be zero at finer scales. This is demonstrated as below. The DWT of the function $f(x)$ at a scale $j \in \mathbb{Z}$ is obtained by the sampling of the CWT as

$$W_d f(k, j) = W_c f(2^{-j}k, 2^{-j}) \tag{4.13}$$

Substituting in the above equation from equation(4.11) , we get

$$W_d f(k, j) = \psi^1(\frac{2^{-j}k - a}{2^{-j}}) = \psi^1(k - 2^j a) \tag{4.14}$$

In the collage error, the block boundaries occur at regular intervals. We will now consider the effect of a particular step edge, that appears at $a = \frac{2l+1}{2^m}$ for some $l, m \in \mathbb{Z}$. It is to be noted that any value of $a \in R+$ can be represented in the above fashion; for some value of l and m. We would like the effect of this edge, to be restricted to the scale m of the DWT. From equation (4.14), the DWT of this edge is given as

$$W_d f(k, j) = \psi^1(k - 2^{(j-m)}(2l + 1)) \tag{4.15}$$

Now suppose that the function $\psi^1(x)$ has its peak value at some $x = x_1$. It is desired that some DWT coefficient at the scale $m - 1$ captures this peak value. For this to happen, the condition to be satisfied for some $k = k_1$ is,

$$k_1 - (2l + 1)/2 = x_1 \iff x_1 = \frac{(2n+1)}{2}, \text{ for some } n \in \mathbb{Z}. \tag{4.16}$$

It is also desirable that only one DWT coefficient, at scale $m - 1$, has a non zero value due to this edge. This in turn implies,

$$f(k - (2l + 1)/2) = 0, \forall k \neq k_1. \tag{4.17}$$

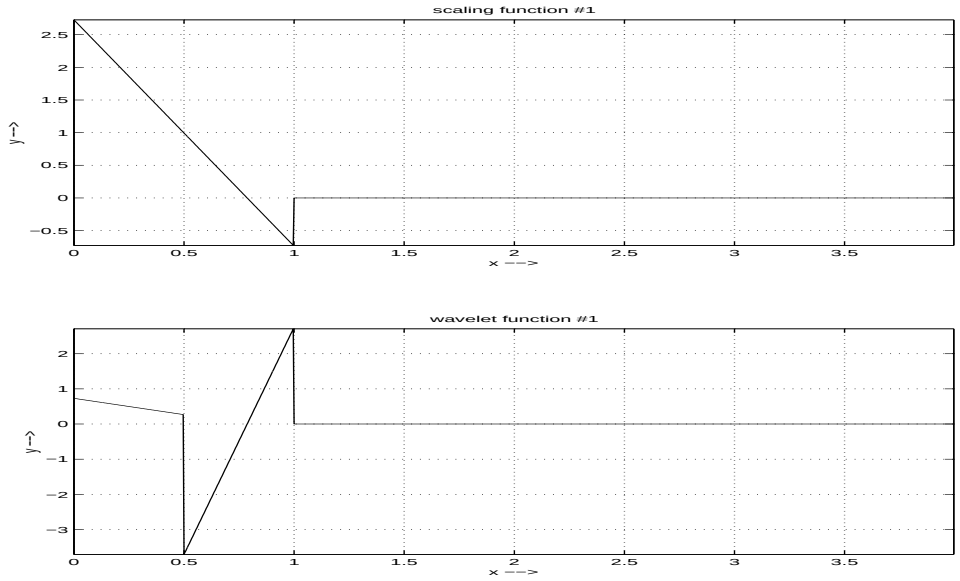

Figure 4.1: Haar Multi-scaling function and wavelet:1

For the DWT coefficients at all scales $l \geq m$ to vanish, we need

$$\psi^1(k - 2^r(2l+1) = 0, \ \forall r \in N, \ \forall k \in Z \tag{4.18}$$

The desirable conditions (4.16), (4.17) and (4.18) together imply

$$\begin{aligned} \psi^1(k) &= 0, \qquad \forall k \in Z. \\ \psi^1(k_1/2) &= 1, \quad k_1 \in Z. \\ \psi^1(k/2) &= 0, \quad \forall k \neq k_1, \ k \in Z. \end{aligned} \tag{4.19}$$

From the above discussion, it is clear that if a function $\psi^1(x)$ which satisfies the above conditions exists, the corresponding DWT will have only one non zero coefficient at scale $m-1$ and all the other coefficients at the higher scales are zeros, for an edge at $a = \frac{2l+1}{2^m}$. It can be seen that the *sinc* function is a function which satisfies the above conditions(4.19) and hence its differential is a good choice for the wavelet. But the support of this function is infinite and hence the mask required. Another function which satisfies the above condition is the *hat* function. This choice corresponds to the *Haar* wavelet. The Haar wavelet at the $(m-1)^{th}$ scale has an edge at $a = \frac{2l+1}{2^m}$ and hence can take care of the edge using a single function.

The Haar function, though it represents the edges well, suffers from a low approximation order. The approximation order can be increased by going for a multi-wavelet extension of the Haar function. The 2^{nd} order extension has scaling functions

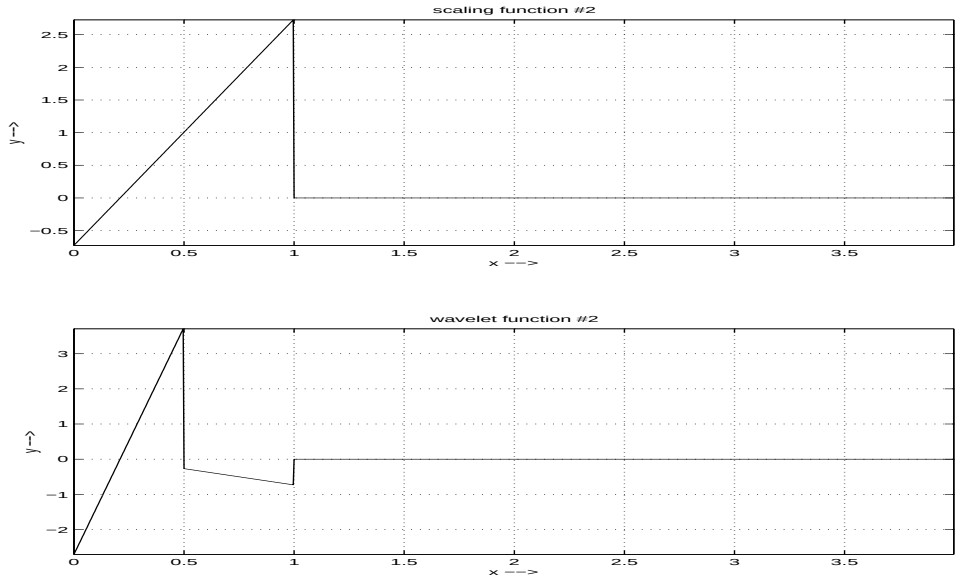

Figure 4.2: Haar Multi-scaling function and wavelet:2

and wavelets as in figures (4.1) and (4.2).

As the 2^{nd} order Haar multi-wavelet has the above mentioned desirable properties and has an approximation order of 2, we choose it for the representation of the collage error. It is to be noted that the functions $\psi_1^1(x)$ and $\psi_2^1(x)$, corresponding to the multi-wavelet basis, have sharper peaks as compared to the hat function, and hence the wavelet coefficients at scale $j < m$ corresponding to an edge at $a = \frac{2l+1}{2^m}$, are smaller than in the Haar wavelet basis. This implies that the effect of edges gets localised more to a particular scale.

4.5 The Method

Usually, to represent a 2-D signal on a wavelet basis, we assume the 2-D wavelet transform to be separable(*i.e.* we assume the 2-D basis as the product of the 1-D basis functions). Here also, we assume the 2-D wavelet basis as a separable basis, where the 1-D basis functions are the Haar multi-wavelet basis. Thus the basis of the representation at a particular scale is obtained as the product of the 1-D Haar multi-scaling functions as shown in figure(4.3).

As mentioned in section(4.3), the isomorphism from $B(I_M)$ to B is determined by the choice of the parameter vectors N and S. For simplicity of implementation, we assume N to be fixed(*i.e.* we assume the domain corresponding to a range block as

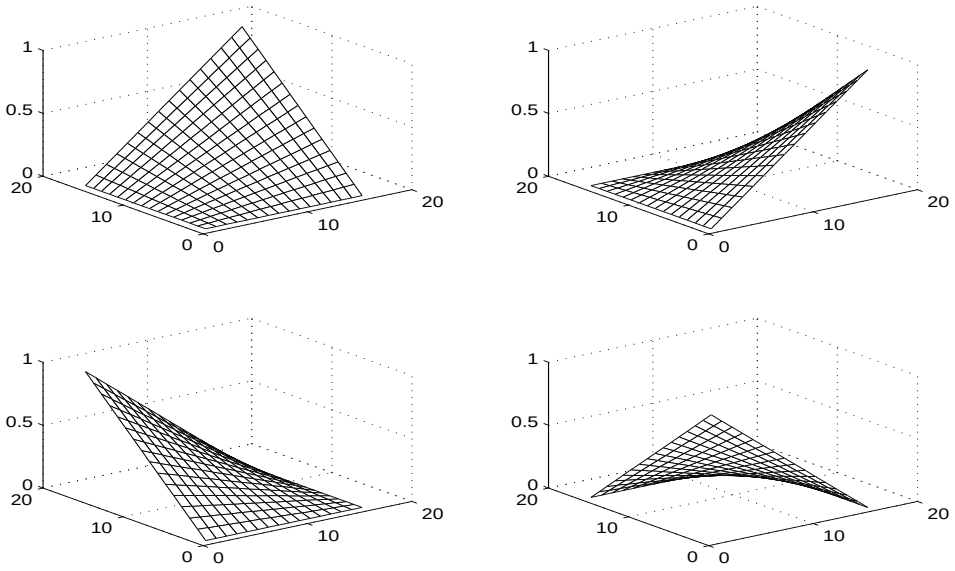

Figure 4.3: Separable 2-D Basis functions implied by the Haar multi-scaling function.

its parent block). The parameter S can be varied so that the projection of λ onto a particular resolution space of the wavelet multi-resolution representation is maximised. The optimal parameter s_i is obtained for each range block independently as the solution of a system of linear equations. The system of linear equation arises in minimising the energy of the projection of λ_i onto the kernel space of the projection operator, which projects λ_i to the particular resolution space.

The collage error is now encoded using the above mentioned wavelet basis. As the block edges in the collage error are represented at a lower scale itself, the wavelet coefficients at a finer scale can be thresholded and can be neglected without the block edge details being lost. The significant coefficients at the finer scales are retained and the collage error is reconstructed from these coefficients. From this approximation of collage error, an approximation of the actual signal is reconstructed by the iteration of the IFS. As desired, the wavelet transform separates those portions of the error which have different perceptual implications to different bands so that we can have an efficient encoding scheme with minimal perceptual disturbance. We choose a simple scheme in which the DWT is weighted using an appropriate weighing function before it is thresholded so that the coefficients corresponding to coarser scales are preferred.

In BFT, three parameters were allocated to each block irrespective of the amplitude of the block edges. If two neighboring blocks have almost the same value for s_i the block edges may not have large discontinuities. In such cases, the number of

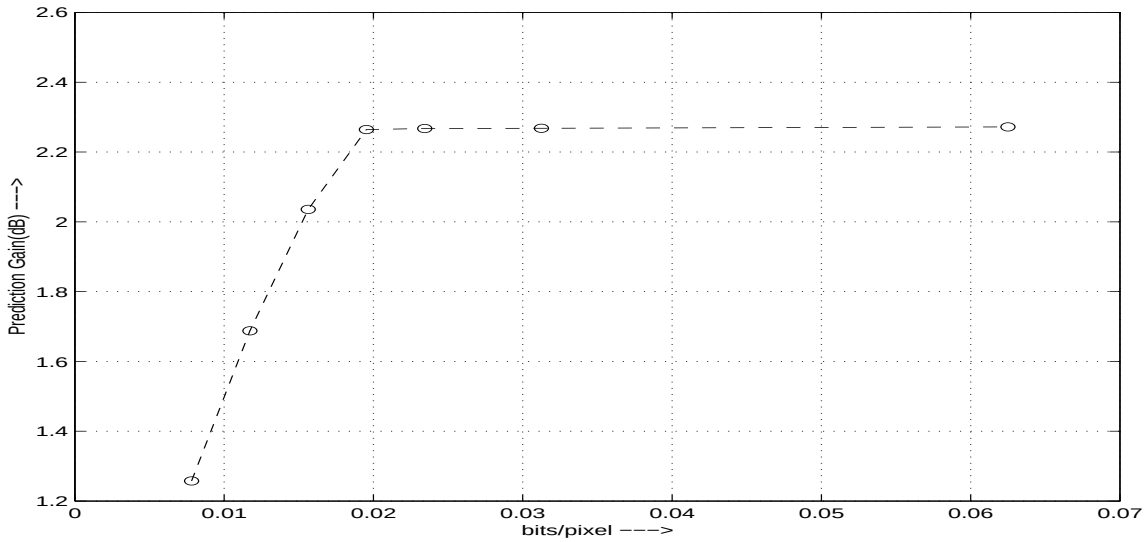

Figure 4.4: Prediction Gain Vs bits/pixel in the representation of s_i; Block size -16x16

parameters in such areas can be reduced in the representation of the error. To accommodate this feature, the collage error is decomposed to a coarser scale and bits are allocated to the wavelet coefficients corresponding to the block edges only if they are above a certain threshold. In doing so, the bits which were wasted in BFT for the representation of almost smooth block edges can be used for the representation of the fine features, thereby increasing the fidelity.

The parameters s_i are encoded using a μ-law quantizer at five bits per parameter. This is because the prediction gain Vs no of bits/parameter saturates at this value as shown in figure(4.4).

The retained wavelet coefficients are also quantised using μ-law . The number of levels for the scaling function coefficients and that of the wavelet coefficients are chosen to be different.

4.6 Simulation Results

The approximation of the collage error signal by truncated DWT, using the Haar multi-filter, represents the block edges better at the cost of the fine details of the signal. Hence the choice of SQNR as a figure of merit is not appropriate, as SQNR does not distinguish between block edges and fine details. So, for the purpose of comparison between the conventional wavelet compression techniques and the Haar multi-wavelet

scheme, we consider a scan line of the Collage error signal. The signal is decomposed to 5 levels using both the cases; The details of levels greater than 3 are neglected and the signal is reconstructed . It can be seen from figures(**??**) and (**??**), which correspond to two portions of the error signal zoomed, that the signal reconstructed using the Haar multi-wavelet represents the edges much better than the Daubechies-2 uniwavelet. The comparison is valid as both have an approximation order of 2. It is also to be noted that in regions where there are fine fluctuations, the Daubechies-2 is marginally better.

In the actual situation, however the Daubechies-2 wavelet is likely to behave slightly better, as we use thresholding of the coefficients, rather than truncation of DWT as before. The decoded image at different compression ratios are shown in figures(**??**) - (**??**). Figures(**??**) - (4.13) and (**??**) - (**??**) shows the decoded images at the same compression ratio, but the wavelet decomposition being taken to different levels. From these figures it can be seen that this scheme fail to capture the crisp edges in the signal (eg. The shoulder of Lena) when we decompose the error signal upto the 5^{th} level. But as we threshold the wavelet coefficents for compression, this scheme (with decomposition upto 5 levels) fail to capture the smooth block edges of the image (eg. The bars in the Lena image exhibiting blockiness), leading to blockiness in those areas. As the degradation of the crisp edges in the image as seen in figure(**??**) is a disturbing artifact, the decomposition upto the 5^{th} level is a preferred scheme. It can be seen that the quality of the baboon image degrades much faster, as the compression ratio is increased, as compared to the Lena image. This is due to the low amount of redundancy present in that image and hence more information is present in the fine detail coefficients.

4.7 Conclusion

The encoding of the collage error using the wavelet introduced, provides an easy alternative for adaptive subdivision (reducing the range block size in areas of higher complexity). It is also very flexible as compared to BFT. As the transform separates the information present in the error signal, that has different perceptual implications, into different bands, perceptual weighting becomes more easy.

The above technique also makes the fractal image compression scheme scalable, making it possible for the signal to be observed at different resolutions.

Chapter 5

Signal Optimised Wavelets

5.1 Introduction

Wavelet Transform Coding is a popular technique adopted for the coding of natural images. As in any other transform coding technique, we try to remove the linear redundancies in the signal, for a possible coding gain. The linear redundancies varies from signal to signal, and hence the transform to be used for the redundancy removal has to be varied from signal to signal for a better coding gain. Adaptation of a transform to the local characteristics of the signal is also a desirable aspect, but due to the large overhead involved(transmission of the basis vectors), this is not a preferred scheme. However in the Wavelet Transforms, as the basis vectors are related to each other , it is ideally suited for adaptive signal coding. Hence the optimisation of wavelets to the local characteristics of a signal is an issue to be resolved.

As coding gain is proportional to the energy compaction in the transform domain, a wavelet transform Optimised to a signal , should approximate the signal better at a particular scale, as compared to other wavelets.

This issue was dealt indirectly by Daubechies[11], where she develops a class of orthogonal wavelets with arbitrarily high approximation orders. A wavelet with an approximation order of N has got the space of piecewise polynomials of order N , as the subspace of the space spanned by the translates of its scaling functions (A particular resolution space). This scheme performs well for signals that are sufficiently smooth which can be approximated well as polynomials of order N. In this scheme, the approximation order is increased at the cost of the support of the wavelet, which

is desired to be small. It is to be noted that the piecewise polynomial space is only a subspace of a particular resolution space and the signal to be coded might not have any components of appreciable energy in the compliment subspace. So it is desired to generate wavelets optimized directly to the signal.

The optimisation of the uni-wavelets to a given signal is dealt with by Tewfick et al. in [1]. In the above paper, the authors parameterise wavelets and pose the problem as a non-linear optimisation problem, where the cost function is the energy of the error in a signal being represented at a particular resolution of the wavelet implied by the above mentioned parameters . They also deal with a suboptimal scheme where the upper bound of the error is minimised rather than the error itself, to reduce the computational complexity.

As mentioned in the previous chapters, multi-wavelets do have certain desirable characteristics as compared to the uni-wavelets. In this chapter, we discuss a scheme to optimise a multi-wavelet to a given signal. As the uni-wavelet being a special case of the multi-wavelets, this scheme is applicable to uni-wavelets too. In this scheme , our search space is not the complete space of multi-wavelets, but a particular subclass of it. This scheme is that way a suboptimal scheme. We assume the given signal to be piecewise fractal in nature(*i.e.* generated by a fractal interpolation functions with piecewise polynomials as lift functions). The entire discussion in this chapter is based on the scheme of generation of multi-wavelets discussed by Geronimo et al[15], [5], [7]. The next section briefly discusses on the this scheme.

5.2 Fractal Interpolation functions and Wavelets

Consider the dilation operator $D_N : B_c(R) \rightarrow B_c(R)$ and the translation operator $T : B_c(R) \rightarrow B_c(R)$ defined as below.

$$D_N f = f(./N), \tag{5.1}$$

$$Tf = f(. - 1) \tag{5.2}$$

Linear spaces that are invariant under the operators D_N and T (eg. function spaces generated by integer translates of a single scaling function) define a multi-resolution

analysis. The spaces F consisting of piecewise fractal interpolation functions , suggested by Barnsley [16] , which satisfy the dilation equations of the form

$$f(u_i(x-n)+n) = \lambda_{n,i}(x-n) + s_{n,i}f(x) \tag{5.3}$$

for $x \in (n, n+1)$ and $i = 0, 1, \ldots, N-1$, where $u_i(x) = (x+i)/N$ and $\lambda_{n,i}(x)$ is an affine function of x and $|max(s_{n,i})| < 1$ are invariant to the operators D_N and T, and hence imply a multi-resolution analysis .

A contractive mapping which converges to the above function was also defined as,

$$(\Phi f_n)(x) = \lambda_{n,i}(u_i^{-1}(x)) + s f_n(u_i^{-1}(x)), \tag{5.4}$$

for all $x \in u_i([0,1]), i = 1, 2, \ldots, N$ and $f_n = f(x-n)|_{[0,1)}$.

Let $B(I)$ denote the Banach space of bounded real valued functions on $I = [0,1)$ with the sup-norm and $B = \bigotimes_{j=0}^{N-1} B(I)$ its N-fold direct product. Let $\lambda_n = (\lambda_{n,0}, \lambda_{n,1}, \ldots, \lambda_{n,N-1}) \in B$. We call the space $\lambda \in B(I)$ as the lift space denoted as Λ.

Corresponding to each $\lambda_n \in B$, for a fixed value of $s_{i,n}$, $i = 0, 1, \ldots, N-1$, we have a $f_n \in B(I)$. The following theorem [5] gives the basic correspondence between the two spaces mentioned above.

Theorem 5.2.1 *The mapping $\lambda \xrightarrow{\theta} f_\lambda$ is a linear isomorphism from B to $B(I)$.*

The theorem implies that the dimensionality of the above mentioned spaces are the same, and hence the number of basis vectors required for the representation are the same. In the above theorem, the parameters s_i are assumed to be constants. It is to be noted that the isomorphism θ mentioned in the above theorem implies an isomorphism $\Theta : \bigotimes_Z B \to \bigotimes_Z B(I)$. The next theorem [5], shows the correspondence between D_N as defined in equation(5.1) and $\Delta_N : \bigotimes_Z B \to \bigotimes B$ defined as below.

$$(\Delta_N \lambda)_{Nn+j} = \lambda_{n,j}, \quad \text{where } \lambda_{i,j} \text{ is defined as} \tag{5.5}$$

$$\lambda_{i,j}(x) = (\lambda_i \; o \; u_j + (s_i\lambda_j - s_j\lambda_i))(x) \tag{5.6}$$

Theorem 5.2.2 *The following diagram commutes:*

$$\begin{array}{ccc} \bigotimes_Z B & \xrightarrow{\Delta_N} & \bigotimes_Z B \\ \downarrow \theta & & \downarrow \theta \end{array}$$

$$\begin{array}{ccc} \bigotimes_Z B_c(R) & & \bigotimes_Z B_c(R) \\ \downarrow \tau & & \downarrow \tau \\ B_c(R) & \xrightarrow{D_N} & B_c(R) \end{array} \tag{5.7}$$

where $\tau : \bigotimes_Z B(I) \to B_c(R)$ does the following mapping.

$$f \xrightarrow{\tau} \Sigma_{n \in Z} f_n(. - n)\chi_{[n,n+1)}, \tag{5.8}$$

where χ_A is the characteristic function of $A \subseteq R$.

The other fundamental operator in $B_c(R)$ is the translation operator T as defined in equation(5.2). It is the operator in the lift space corresponding to the operator T is the right shift operator $\sigma : \bigotimes_Z B \longrightarrow \bigotimes_Z B$ given by

$$\{\lambda_n\}_{n \in Z} \longrightarrow \{\lambda_{n-1}\}_{n \in Z} \tag{5.9}$$

The above two theorems along with equation(5.9) prove that the space of piecewise fractal interpolation functions given by equation(5.8) are invariant to the operators T and D_N.

Till now the elements of the lift space Λ were arbitary elements of $B(I)$. But the elements being defined arbitarly causes the attractor function as defined in equation(5.8) to be highly discontinuous. As this space of attractor functions forms a particular resolution space of the MRA defined by the above scheme, this space is desired to span the space of $C^r(R)$ functions. The theorem given below [5] gives the condition for which this happens.

Suppose the operators $L_i^m(\lambda_0)$, $\hat{L}^m(\lambda_0)$ be given as

$$L_i^m \lambda = (1 - sN^m)\left(\lambda_{0,i}^m(0) - \lambda_{0,i-1}^m(1)\right) + (sN^m)\left(\lambda_{0,0}^m(0) - \lambda_{0,N-1}^m(1)\right) \tag{5.10}$$

$$\hat{L}^m \lambda = \left(\lambda_{0,0}^m(0) - \lambda_{-1,N-1}^m(1^-)\right) \tag{5.11}$$

Let ζ^r be the set of all λ which satisfies the below given equation for all values of n.

$$\sigma^n \lambda \in \bigcap_{m=0}^{r} \left(\left(\bigcap_{i=1}^{N-1} Ker(L_i^m) \right) \cap Ker(\hat{(L)}^m \right) \tag{5.12}$$

Theorem 5.2.3 *Suppose that* $|s|N^r < 1$. *Then* $(\tau \ o \ \theta)^{-1} C^r(R) = \zeta^r$.

This theorem gives the sufficient condition on the space of functions Λ so that the

space of piecewise fractal interpolation functions given by equation(5.8) are r times continuously differentiable.

From the above theorems, we find that the space of piecewise fractal interpolation functions(FIF) are dilation and translation invariant, and under the conditions of the theorem 5.2.3, they are r times continuously differentiable also. The next problem is the construction of the scaling functions so that the above mentioned space becomes a particular resolution space of the implied MRA. We discuss the issue of optimising the above mentioned space to the given signal.

In the above section, the space Λ was considered to be $B(I)$. If it is so, corresponding to any arbitary function $f \in B_c(R)$, we have a $\lambda \in \bigotimes_Z B(I)$ by theorem 5.2.1. As the dimensionality of such a Λ space is infinity and so is the number of basis functions required to represent such a space.

So the space Λ is restricted as $\Pi_n^r = \Pi_n \cap \zeta^r$, and N is chosen to be 2, where $\Pi_n = \bigotimes_Z \left(\bigotimes_{j=0}^{j=1} \pi_n \right)$ and π_n is the set of all n^{th} order polynomials, whose domain is $[0, 1)$. For simplicity, n is set as 1, and r as 1. It is to be noted that the dimension of the space of functions $\Pi_1^1 . \chi_{[0,1)}$ is three, and so is the dimension of the space of functions $f . \chi_{[0,1)}$. Hence we need three functions to span the space of functions $f . \chi_{[0,1)}$. So to span the entire space of functions whose domain is R, we need the translates of two functions, which are the scaling functions. This is because the continuity constraint at the integer points further reduces the dimension by one.

As mentioned in [7], such a function $f . \chi_{[0,1)}$, is characterised uniquely by its values at $0, \frac{1}{2}, 1^-$. Suppose the value of a function at these points are given by the vector y. As the function is defined uniquely by this vector, we can call a particular vector in this class as f_y. So the basis functions of this space can be given as $f_{y_0}, f_{y_1}, f_{y_2}$, where y_0, y_1, y_2 correspond to some arbitary basis in R^3. Let this basis be the vectors $y_0 = (1, q, 0),\ y_1 = (0, 1, 0)$ & $y_2 = (0, p, 1)$. From the basis functions $f_{y_0}, f_{y_1}, f_{y_2}$, we can generate the basis for the FIF space(scaling function) as given below.

$$\hat{\phi}_0(x) = \begin{cases} f_{y_1}(x) & x \in [0, 1) \\ 0 & \text{elsewhere} \end{cases} \tag{5.13}$$

$$\hat{\phi}_1(x) = \begin{cases} f_{y_2}(x) & x \in [0, 1) \\ f_{y_0}(x - 1) & x \in [1, 2) \\ 0 & \text{elsewhere} \end{cases} \tag{5.14}$$

and the normalised scaling function $\phi_i(x)$ is given by,

$$\phi_i(x) = \frac{\hat{\phi}_i(x)}{||\hat{\phi}_i(x)||} \tag{5.15}$$

For the scaling functions to be orthonormal, by [7] we have,

$$p = \frac{-(4-6s_0-2s_1s_0-4s_0^2-4s_1^2+3s_0^3+3s_0^2s_1)}{16+4s_0s_1-4s_0^2-4s_1^2} \tag{5.16}$$

$$q = \frac{-(4-6s_1-2s_1s_0-4s_0^2-4s_1^2+3s_1^3+3s_1^2s_0)}{16+4s_0s_1-4s_0^2-4s_1^2} \quad \text{and,} \tag{5.17}$$

$$\begin{aligned} g(s_0,s_1) &= 2s_1^4+6s_1^3-7s_1^3s_0+18s_1^2s_0-28s_1^2-7s_1s_0^3+18s_1s_0^2 \\ &\quad -14s_1s_0+12s_1+s_0^4+6s_0^3-28s_0^2+12s_0+8 = 0 \end{aligned} \tag{5.18}$$

5.3 Optimising the FIF space to the signal

As we constrain the Λ space as Π_n^r, we are restricting the set of possible functions in the FIF space. Hence every function in $B_c(R)$ will not have such a representation, as in the case where the Λ space was the entire Banach space. So now the representation becomes an approximation and the FIF space defines a multi-resolution space in the natural way. As mentioned above, we have to look for a better approximation of the signal at a lower scale itself. In other words, we have to optimise the FIF space to the signal space.

This approximation can be seen as below. The given function $f \in B_c(R)$, by the isomorphism θ^{-1}, which in turn is defined by the parameters s_0 & s_1 maps the signal onto $\lambda \in \Lambda$ as given by the theorem(5.2.1). It should be noted that the Λ space here refers to the entire $B_c(R)$ space and not the space Π_n^r. Now the mapped function is projected onto the Π_n^r space. The quality of the approximation indeed depends on the projection of λ onto the Π_n^r space. So it is desired that the given function is mapped onto a λ whose projection onto the Π_n^r space is a maximum. This is done by varying the isomorphism θ^{-1}, which is parameterised by s_0 & s_1 . Hence, the formulation of the problem becomes similar to that in chapter 4.

5.3.1 The Method

The minimisation of the error in the projection of $\theta^{-1}(f)$ to the Π_n^r space is posed as

- A constrained Non-linear optimisation scheme, where the constraint is the orthogonality constraint defined by equation(5.18). In this case, the solution will be an orthogonal multi-resolution space spanned by two scaling functions. The scaling functions are obtained from equations (5.13), (5.14) & (5.15). The functions $f_{y_0}, f_{y_1}, f_{y_2}$ are uniquely specified by p & q values defined by equations(5.16) & (5.17).
- An unconstrained optimisation scheme, where the orthogonality constraint is not imposed. In this case we can get closed form expressions for the optimal parameters s_0 & s_1,. This scheme gives a bi-orthogonal multi-resolution space, where the scaling functions are given still by (5.13), (5.14) & (5.15). But here the parameters p & q can be set arbitarly. We set these values to be $\frac{1}{2}$, so that the scaling functions will be more smoother.

It was shown above that the spaces form an MRA, and hence the basis functions of a particular resolution space (scaling functions) will satisfy the two scale relationship given as

$$\Phi(x) = \Sigma_{i=0}^{3} C_i \Phi(2x - i) \text{ , where} \tag{5.19}$$

$$\Phi(x) = \begin{bmatrix} \phi_0(x) \\ \phi_1(x) \end{bmatrix} \tag{5.20}$$

Now the multi-filter coefficients C_i can be easily found out, by solving the equation(5.19), at $x = i/4,\ i = 1, 2 \ldots, 8$. The values of $\Phi(x)$ at these points are obtained from the scaling function values at these points, which in turn are characterised $y_0,\ y_1,\ y_2$ and the parameters s_0 & s_1.

To have the complete MRA decomposition of $L^2(R)$ we need the multi-filter corresponding to the wavelet part also. In the case of orthogonal MRA, these parameters might be found out using the algorithm mentioned in [8]. This part was not attempted.

It is to be noted that in the unconstrained optimisation scheme, the problem becomes very similar to the scheme in chapter 4.

4^{th} level

5.4 Simulation Results

Both the schemes were tried out on three sets of data. They are

- The sound of a bell ringing. This is a highly harmonic sound. The results are given in figure (**??**)& (**??**).
- The utterance of the vowels "aaeeuu". This, being a voiced sound, has predominant amplitude in the frequency domain around the formant frequencies. The simulation results are as in figures (**??**)& (**??**).
- The utterance of the unvoiced sound "sshhh". This sound is a broad band sound and is supposed to have some *fractal* nature as it is generated by turbulence of air. The results are in plots (**??**)& (**??**).

The results as given in the plots correspond to the scheme being optimised to 4^{th} and 5^{th} levels of decomposition respectively. It can be seen from the plots that the optimal coefficients are scattered along the line joining (-0. 2, -0. 2) and (0, 0) in the first four plots. This line corresponds to the parameters for which the multi-wavelets are symmetric(ie. the filters are linear phase). This indicates that , for a better approximation at a lower scale, symmetry of the wavelet is a desired condition in the case of harmonic sources.

It can also be observed that in the first two cases, the optimal coefficents drift towards the point (-0. 2, -0. 2) as the levels of decomposition is increased(ie. at higher compression ratios). This is expected as for harmonic sources, a smooth approximation is always better as compared to rough ones(which arises if the points are far from the above mentioned point). But in the case of unvoiced sounds, the parameter values does not change much, as the levels of decomposition is increased. This can be seen from the plots (**??**)& (**??**), and is justified by the fractal nature of turbulent sounds. The high values of the coefficents implies a high amount of self similarity.

It is to be noted that solid curve is the one corresponding to the zeros of the orthogonality constraint imposed by equation(5.18). It can be seen from the plots (**??**)& (**??**), that when the orthogonality constraint is imposed, the optimal points drift towards (-0. 2, -0. 2). In these cases the orthogonality constraint is a severe constraint that it takes the parameters far away from optimality. In such cases bi-orthogonal multi-wavelets is a good choice for better approximation of such signals. It is to be noted that as the continuity constraint is imposed, the absolute value of the optimal coefficents are upper bounded by 1.

5.5 Conclusion

The optimisation of multi-wavelets to a given signal is the theme of this chapter. The signals were assumed to be piecewise fractal in nature, generated by fractal interpolation functions, and the wavelets were optimised to span this class of functions.

By simulations it was found that for harmonic sounds, wavelets that are smooth are more optimal as compared to rough ones. So, a high approximation order is desired in the representation of harmonic sounds. It is also seen that for harmonic sounds, symmetry of the wavelets is also a desired character, as the optimal coefficents are seen to cluster along the line corresponding to symmetric multi-wavelets.

However, for unvoiced sounds generated by turbulence of air, has some self-similarity, that is indicated by high values of the coefficents. In these cases the desired multi-wavelets are bi-orthogonal ones as the orthogonality imposes a serious constraint, which makes the system drift from optimality.

Chapter 6

Conclusions

The main focus of this thesis was on optimising wavelets to a given signal. The aim was to generate optimal wavelet basis for signal compression, that would yield higher compression ratios. We assumed that a wavelet is optimal for the representation of a signal, if the projection of the signal to a particular resolution of the wavelet basis, is a better approximation to the signal as compared to the projection to the corresponding space of other wavelet bases.

In Chapter 3 we explored on a possible extension to the conventional Multi-Resolution Analysis. The aim was to look for a wavelet basis that is more regular for a particular support length. The new MR axioms were stated, and a filter bank structure that satisfies the new axioms were suggested. But it was found that when the orthogonality constraint is imposed, the wavelets ceased to have even the first order approximation property. If the above constraint was not imposed, the wavelets have the desired properties - short support and high approximation orders.But later it was observed that the new wavelet bases form a special case of a more general class of multi-wavelet bases. As the new class of wavelets are highly irregular (high fractal dimension), probably they might be optimal for the representation of more fractal signals.

In Chapter 4 we introduced a new multi-wavelet basis for the encoding of collage error in a Fractal Image Compression scheme. This basis will restrict the information corresponding to the block edges, intrinsic in the collage error(as we assume the signal to be block-wise fractal), to the lower resolution spaces of the wavelet decomposition. Conventional smooth wavelets smear this information to all scales. This information of the block edges, if not represented, will lead to blockiness in the reconstructed image which is a very disturbing artifact. The loss of fine details of the image will not be as disturbing as blockiness. As the new transform separates the information present in the signal that has different perceptual implications to different bands, the ease of applying a perceptual criterion in the encoding of

the error becomes easy. In the new scheme,the thresholding of the wavelet coefficients, which is a commonly used scheme in transform coding, becomes a simpler alternative to adaptive subdivision which is used in conventional fractal image coding.

In the above scheme, we reconstructed the collage error from the retained wavelet coefficients and iterated the IFS to yield the attractor which is an approximation to the signal. The iteration generates fine scale details from coarse scale coefficients. Hence a scheme can be thought of where we incorporate the iteration also to be performed by using a new reconstruction strategy.

The optimisation of multi-wavelets to a given signal is the central theme of the Chapter 5. The signals were assumed to be piecewise fractal interpolation functions and the multi-wavelet basis is optimised to span this space. In this scheme, we restricted the search space to be a subclass of the entire multi-wavelet family. Simulation results on speech shows that for vowel sounds, which are almost harmonic in nature, the GHM wavelets are almost optimal. However for fricative sounds, that are generated due to the turbulence of air, multi-wavelets which are biorthogonal in nature are better suited. For the representation of all class of signals , symmetry seems to be a requirement for optimality. We derive a scheme to find out the low-pass mask of the scaling function. However the complete filter bank structure and the derivation of the high-pass filters from this mask are yet to be investigated.

Appendix A

Some results used in Chapter 3

A.1 To show that the $u_j \perp w_j \Rightarrow$ equation (3.16).

Consider an arbitrary function $f(x) \in u_0$ .It can be represented as

$$f(x) = \sum_{k=-\infty}^{\infty} a_k \eta(\frac{x}{4} - k)$$

for some set of coefficients $(a_k, k \in Z)$.

Taking the Fourier transform of both the sides we get,

$$\begin{aligned} \hat{f}(\omega) &= A(4\omega)\hat{\eta}(4\omega) \\ &= A(4\omega)D(\omega)\hat{\phi}(\omega) \end{aligned} \tag{A.1}$$

where $A(\omega)$ is the discrete Fourier transform of the sequence $(a_k, k \in Z)$

By the assumption $u_j \perp w_j$ we have $f(x)$ orthogonal to every basis vector of w_0. *ie* to $(\gamma(-1,k)(x), \forall k \in Z)$. This has to hold good for all $f(x) \in u_0$. All possible functions in u_0 being orthogonal to one basis vector of w_0 implies that they are orthogonal to all the basis vectors of w_0.

From (3.12) ,the Fourier transform of the basis vector $\gamma(\frac{x}{2})$ is given by

$$\hat{\gamma}(\omega) = C(\omega).\hat{\phi}(\omega) \tag{A.2}$$

Let $S : \hat{V_0} \rightarrow L^2[0, 2\pi]$ be the unitary operator given by

$$S(A(\omega)\hat{\phi}(\omega)) = A(\omega)$$

To show that $\hat{f}(\omega)$ is orthogonal to $\hat{\gamma}(2\omega)$,it is sufficient to show that $S(\hat{f}(\omega))$ is orthogonal to $S(\hat{\gamma}(2\omega))$, as S being unitary. Hence,

$$\int_0^{2\pi} A(4\omega)D(\omega)\overline{C}(\omega)d\omega = 0 \quad \Rightarrow$$

$$\int_0^{2\pi} A(4\omega)[D(\omega)\overline{C}(\omega) + D(\omega+\tfrac{\pi}{2})\overline{C}(\omega+\tfrac{\pi}{2}) + D(\omega+\pi)\overline{C}(\omega+\pi) + D(\omega+\tfrac{3\pi}{4})\overline{C}(\omega+\tfrac{3\pi}{4})]d\omega = 0$$

As the above equation has to hold for all $A(\omega)$, the above equation implies

$$[D(\omega)\overline{C}(\omega) + D(\omega+\frac{\pi}{2})\overline{C}(\omega+\frac{\pi}{2}) + D(\omega+\pi)\overline{C}(\omega+\pi) + D(\omega+\frac{3\pi}{4})\overline{C}(\omega+\frac{3\pi}{4})] = 0 \tag{A.3}$$

The above equation will be satisfied if

$$D(\omega)\overline{C}(\omega) + D(\omega+\pi)\overline{C}(\omega+\pi) = 0 \quad ,\forall\omega$$

$$\Rightarrow \frac{D(\omega)}{D(\omega+\pi)} = -\frac{\overline{C}(\omega+\pi)}{\overline{C}(\omega)} \tag{A.4}$$

This in-turn implies that there exists a π periodic function $\alpha(\omega)$ such that

$$D(\omega) = \alpha(\omega)\overline{C}(\omega+\pi) \tag{A.5}$$

A.2 To show that the cross terms in equation(3.18) vanish if equation(3.16) and equation(3.19) hold.

Consider the third term of the equation (3.18).It can be shown to be zero as shown below.

$$\sum_m \sum_p c_m d_p < \phi(2x-2k-m), \phi(4x-4l-p) > \;=$$
$$\sum_m c_m < \phi(2x-2k-m), \sum_p d_p \phi(4x-4l-p) > \;=$$
$$\sum_m c_m < \phi(2x-2k-m), \eta(x-l) >$$

By using equation (3.11),the above equation reduces to

$$\sum_m c_m < \eta(2x-2k-m), \eta(x-l) > \;\; = \;\; 0$$

This is because $\eta(x-l)$ is a basis function of u_2 and $\gamma(2x-2k-m)$ is a basis function of w_1,,which are orthogonal spaces .Now substituting for $\eta(x-l)$ from equation (3.12) and by a similar argument ,the above equation reduces to

$$\sum_m \sum_p c_m d_p < \eta(2x-2k-m), \eta(4x-4l-p) > \;\; = \;\; 0$$

Substituting for $\eta(2x-2k-m)$ and $\eta(4x-4l-p)$ in terms of their inverse Fourier transform and reducing we get,

$$\int_{-\infty}^{\infty} C(2\omega) D^*(\omega) \eta(2\omega) \eta(\omega) \exp(-j\omega(4k-4l)) = 0$$

Using the periodicity of $C(2\omega)$,changing the infinite integral to be from 0 - π we get,

$$\int_0^{\pi} C(2\omega)[D^*(\omega) + D^*(\omega+\pi)] \sum_{k=-\infty}^{\infty} [\eta(2\omega+k\pi)\eta(\omega+k\pi)] \exp(-j\omega(4k-4l)) = 0$$

This equation is satisfied if $[D^*(\omega)+D^*(\omega+\pi)] \;=\; 0, \; \forall\omega$. This in-turn implies $\alpha^*(\omega)[C^*(\omega)+ C^*(\omega+\pi)] \;=\; 0$. Hence if the term $C^*(\omega) + C^*(\omega+\pi) \;=\; 0$ the cross term vanish.In similar lines it can be shown that the other cross term also vanishes if the above condition is satisfied. Hence the condition for the cross term to vanish is

$$C(\omega) = -C(\omega+\pi), \forall\omega$$

A.3 To show that equation (3.20) $\Longleftrightarrow$ equation(3.21)

Consider the first term of equation (3.20).

$$\sum_m \sum_o c_m c_o < \phi(2x-2k-m), \phi(2x-2l-o) >$$

Substituting for $\phi(2x-2k-m)$ and $\phi(2x-2l-o)$ by the inverse Fourier transform of $\hat{\phi}(\omega)$ at the corresponding points and then after a little algebra we get,

$$\int_{-\infty}^{\infty} |C(\omega)|^2 |\hat{\phi}(\omega)|^2 \exp(2j\omega(k-l)) d\omega \;\; =$$

$$\int_0^{2\pi} |C(\omega)|^2 \sum_{k=-\infty}^{\infty} |\hat{\phi}(\omega + 2k\pi)|^2 \exp(2j\omega(k-l))d\omega \quad =$$

$$\int_0^{\pi} [|C(\omega)|^2 + |C(\omega+\pi)|^2] \sum_{k=-\infty}^{\infty} |\hat{\phi}(\omega + k\pi)|^2 \exp(2j\omega(k-l))d\omega$$

Substituting for 2ω as ω and by the fact that $< \phi(x-l), \phi(x-k) >= \delta(k,l) \iff \sum_{k=-\infty}^{\infty} |\hat{\phi}(\omega + 2k\pi)|^2 = 1$,we get

$$\int_0^{2\pi} [|C(\frac{\omega}{2})|^2 + |C(\frac{\omega}{2}+\pi)|^2] \exp(j\omega(k-l))d\omega$$

Similarly the last term of equation (3.20) correspond to

$$\int_0^{2\pi} [|D(\frac{\omega}{4})|^2 + |D(\frac{\omega}{4}+\frac{\pi}{2})|^2 + |D(\frac{\omega}{4}+\pi)|^2 + |D(\frac{\omega}{4}+\frac{3\pi}{2})|^2] \quad \exp(j\omega(k-l))d\omega \tag{A.6}$$

Combining the integrals as in equation (3.20) and taking the inverse Fourier transform of both the sides we get,

$$|C(\frac{\omega}{2})|^2 + |C(\frac{\omega}{2}+\pi)|^2 + |D(\frac{\omega}{4})|^2 + |D(\frac{\omega}{4}+\frac{\pi}{2})|^2 + |D(\frac{\omega}{4}+\pi)|^2 + |D(\frac{\omega}{4}+\frac{3\pi}{2})|^2 = 1$$

Bibliography

[1] D. S. Ahmed H.Tewfick and P. Jorgenson, "On the optimal choice of a wavelet for signal representation.," *IEEE Transactions on Information Theory*, pp. 747–782, March 1992.

[2] G. S. Cristopher Heil and V. Strela, "Approximation by translates of refinable functions," *preprint.*

[3] Devore and Jawerith, "Signal compression using wavelet transform coding," *IEEE Transactions on Information Theory*, March 1992.

[4] D.M.Munro and F.Dudbridge, "Fractal approximation of image blocks," *ICASSP*, vol. 3, pp. 485–88, 1995.

[5] B. D.P.Hardin and P.R.Massopust, "Multiresolution analysis based on fractal functions," *Journal of Approximation Theory*, vol. 71, pp. 104–120, 1992.

[6] Y. Fisher, *Fractal Image Compression:Theory and Background.* Springer Verlag, 1995.

[7] D. George Donovan, J.S.Geronimo and P.Massopust, "Construction of orthogonal wavelets using fractal interpolation functions," *SIAM Journal of mathematical Analysis*, vol. 27, pp. 1152–1192, July 1996.

[8] G.Strang and V.Strela, "Short wavelets and matrix dilation equations," *IEEE Transactions on Signal Processing*, vol. 43, pp. 108–114, January 1993.

[9] H. Heijmans, *Wavelets and Multiresolution Analysis.* World Scientific, 1 ed., 1995.

[10] I.Daubechies, "Ten lectures on wavelets," *CBMS-NSF Series in Applied mathematics,SIAM*, no. 61, 1992.

[11] I.Daubechies, "Orthonormal bases of compactly supported wavelets," *Communications on Pure and Applied Mathematics*, vol. 41, pp. 909–996, 1998.

[12] I.Daubechies and Lagarias, "Two scale difference equations i," *SIAM J.Math.Anal.*, vol. 22, pp. 1388–1410, 1991.

[13] I.Daubechies and Lagarias, "Two scale difference equations ii.local regularity,infinite products of matrices and fractals," *SIAM.J.Math.Anal*, vol. 23, pp. 1031–1410, 1992.

[14] B. Jawerith and W. Sweldens, "An overview of wavelet based multiresolution analysis," *SIAM Reveiw*, vol. 36, p. September, 1994 1994.

[15] D. J.S.Geronimo and P.R.Massopust, "Fractal functions and wavelet expansions based on several scaling functions," *Journal of Approximation theory*, vol. 78, pp. 373–401, 1994.

[16] M.Barnsley, *Fractals Everywhere*. Academic Press, 3 ed., 1993.

[17] Stephane.G.Mallat, "Multiresolution approximations and wavelet orthonororormal bases of $l^(r)$," *Transactions on the American Mathematical Society*, September 1989.